

# Disorder-induced trapping versus Anderson localization in Bose-Einstein condensates expanding in disordered potentials

L. Sanchez-Palencia, D. Clément, P. Lugan, P. Bouyer, and A. Aspect

Laboratoire Charles Fabry de l'Institut d'Optique, CNRS and Univ. Paris-Sud, Campus Polytechnique, RD 128, F-91127 Palaiseau cedex, France

**Abstract.** We theoretically investigate the localization of an expanding Bose-Einstein condensate with repulsive atom-atom interactions in a disordered potential. We focus on the regime where the initial inter-atomic interactions dominate over the kinetic energy and the disorder. At equilibrium in a trapping potential and for the considered small disorder, the condensate shows a Thomas-Fermi shape modified by the disorder. When the condensate is released from the trap, a strong suppression of the expansion is obtained in contrast to the situation in a periodic potential with similar characteristics. This effect crucially depends on both the momentum distribution of the expanding BEC and the strength of the disorder. For strong disorder as in the experiments reported by D. Clément *et al.*, Phys. Rev. Lett. **95**, 170409 (2005) and C. Fort *et al.*, Phys. Rev. Lett. **95**, 170410 (2005), the suppression of the expansion results from the fragmentation of the core of the condensate and from classical reflections from large modulations of the disordered potential in the tails of the condensate. We identify the corresponding disorder-induced trapping scenario for which large atom-atom interactions and strong reflections from single modulations of the disordered potential play central roles. For weak disorder, the suppression of the expansion signals the onset of Anderson localization, which is due to multiple scattering from the modulations of the disordered potential. We compute analytically the localized density profile of the condensate and show that the localization crucially depends on the correlation function of the disorder. In particular, for speckle potentials the long-range correlations induce an effective mobility edge in 1D finite systems. Numerical calculations performed in the mean-field approximation support our analysis for both strong and weak disorder.

PACS numbers: 03.75.Kk, 64.60.Cn, 79.60.Ht, 03.75.Hh, 03.75.-b, 05.30.Jp

## Contents

<b>1</b>	<b>Introduction</b>	<b>2</b>
1.1	Disorder and ultracold atomic gases . . . . .	2
1.2	Scope and main results of the paper . . . . .	3
1.3	Organization of the paper . . . . .	4
<b>2</b>	<b>Condensates at equilibrium in a combined harmonic trap plus disordered potential</b>	<b>5</b>
2.1	Interacting Bose-Einstein condensates in a 1D inhomogeneous potential	5
2.2	The Bose-Einstein condensate wavefunction . . . . .	6

<b>3 Strong disorder: Suppression of the expansion of a Bose-Einstein condensate in a speckle potential and disorder-induced trapping scenario</b>	<b>7</b>
3.1 Expansion of an interacting BEC in a speckle potential . . . . .	7
3.2 Scenario of disorder-induced trapping . . . . .	10
3.2.1 Quasi-static Thomas-Fermi profile in the core of the BEC . . .	10
3.2.2 Strong reflections in the tails of the BEC . . . . .	13
3.3 Expansion of a condensate in a periodic potential . . . . .	13
<b>4 Weak disorder: Onset of Anderson localization in the expansion of a condensate</b>	<b>16</b>
4.1 General model of Anderson localization of an expanding Bose-Einstein condensate . . . . .	16
4.2 Anderson localization of an expanding Bose-Einstein condensate in an impurity model of disorder . . . . .	19
4.3 Anderson localization of an expanding Bose-Einstein condensate in a speckle potential . . . . .	20
<b>5 Conclusion and perspectives</b>	<b>21</b>
<b>Appendix A and periodic potentials</b>	<b>24</b>
Appendix A.1 Speckle disordered potential . . . . .	25
Appendix A.2 Impurity model of disorder . . . . .	26
Appendix A.3 Periodic potential . . . . .	27
<b>Appendix B Formalism for the calculation of Lyapunov exponents in 1D disordered potentials with finite-range correlations</b>	<b>27</b>

## 1. Introduction

### 1.1. Disorder and ultracold atomic gases

Understanding the effect of disorder in physical systems is of fundamental importance in various domains, such as mechanics, wave physics, solid-state physics, quantum fluid physics, or atomic physics. Although in many situations this effect is weak and can be ignored in first approximation, it is not always so. Strikingly enough, even arbitrary weak disorder can dramatically change the properties of physical systems and result in a variety of non-intuitive phenomena. Many of them are not yet fully understood. Examples in classical systems include Brownian motion [1], percolation [2], and magnetism in dirty spin systems [3, 4, 5, 6, 7]. In quantum systems the effects of disorder can be particularly strong owing to the complicated interplay of interference, particle-particle interactions and disorder. The paradigmatic example is (strong) Anderson localization of non-interacting particles [8, 9, 10, 11]. Other interesting effects of disorder in quantum systems include weak localization and coherent back-scattering [12], disorder-driven quantum phase transitions and the corresponding Bose glass [13, 14, 15] and spin glass [16, 17] phases.

Anderson localization (AL) signals out in two equivalent ways, either as the suppression of the transport of matterwaves in disordered media, or as an exponential decay at large distances of the envelop of the eigenstates of free-particles in a disordered potential [11]. Both properties strongly contrast with the case of periodic potentials, in

which transport is free and all eigenstates extend over the full system as demonstrated by the Bloch theorem [18]. Anderson localization is due to a destructive interference of particles (waves) which multiply scatter from the modulations of a disordered potential. It is thus expected to occur when interferences play a central role in the multiple scattering process [11]. In three dimensions, it requires the particle wavelength be larger than the scattering mean free path  $l$  as pointed out by Ioffe and Regel [19]. One then finds a mobility edge at momentum  $k = 1/l$ , below which AL can appear. In one and two dimensions all single-particle quantum states are predicted to be localized [20, 21, 22], although for certain types of disorder one has an effective mobility edge in the Born approximation [23, 24, 25].

Ultracold atomic gases are now widely considered to revisit standard problems of condensed matter physics under unique control possibilities. Dilute atomic Bose-Einstein condensates (BEC) [26, 27, 28, 29] and degenerate Fermi gases (DFG) [30, 31, 32, 33, 34] are produced routinely taking advantage of the recent progress in cooling and trapping of neutral atoms [35, 36, 37]. In addition, controlled potentials with no defects, for instance periodic potentials (optical lattices), can be designed in a large variety of geometries [38]. In periodic optical lattices, transport has been widely investigated, showing lattice-induced reduction of mobility [39, 40, 41] and interaction-induced self-trapping [42, 43]. Controlled disordered potentials can also be produced optically as demonstrated in several recent experiments [44, 45, 46, 47, 48], for instance using speckle patterns [49, 50]. Other techniques can be employed to produce controlled disorder such as the use of magnetic traps designed on atomic chips with rough wires [51, 52, 53, 54, 55], the use of localized impurity atoms [56, 57], or the use of radio-frequency fields [58]. However, the use of speckle potentials has unprecedented advantages from both practical and fundamental points of view. First, they are created using simple optical devices and their statistical properties are very well known [59, 60]. Second, they have finite-range correlations which offers richer situations than theoretical  $\delta$ -correlated potentials (*i.e.* uncorrelated disorder) and the correlation functions can be designed almost at will by changing the geometry of the optical devices [59, 60]. Finally, both the amplitude and the correlation length (down to fractions of micrometers) can be controlled accurately and calibrated using ultracold atoms [48].

Within the context of ultracold gases, important theoretical efforts have been devoted to disordered optical lattices which mimic the Hubbard model [14, 61, 62, 63, 64]. For bosons, quantum phase transitions from superfluid to Bose glass and Mott insulator phases have been predicted [65, 66] and evidence of the Bose glass has been obtained experimentally [67]. With Fermi-Bose mixtures, the phase diagram is even richer and include the formation of a Fermi-glass, a quantum percolating phase and a spin glass [68, 69, 70]. Effects of disorder in Bose gases at equilibrium without optical lattice have been addressed in connection with the behavior of the BEC phase transition [71, 72], the quantum states of Bose gases [73, 74, 75, 76], the localization of Bogolyubov quasi-particles [77, 78], the dynamics of time-of-flight imaging of disordered BECs [79, 80], and random-field-induced order in two-component Bose gases [81, 82].

### 1.2. Scope and main results of the paper

The dynamics of BECs in disordered (or quasi-disordered) potentials is also attracting significant attention in a quest for observing Anderson localization in non-interacting

BECs [56, 83, 84] or in BECs with repulsive interactions [25, 85, 86, 87]. Recent experiments have demonstrated the strong suppression of transport in expanding BECs in the presence of optical speckle potentials [45, 46, 48], but this effect is not related to Anderson localization [45].

In this paper, we theoretically and numerically analyze the expansion of an interacting one-dimensional (1D) BEC in a disordered potential. We focus on a regime where the inter-atomic interactions *initially* exceed the kinetic energy (Thomas-Fermi regime), a situation that significantly differs from the textbook Anderson localization problem but which is relevant for almost all current experiments with disordered BECs [45, 46, 47, 48, 79, 80]. We distinguish two regimes that we name *strong disorder* and *weak disorder* respectively.

The case of strong disorder corresponds to the situation of the experiments of Refs. [45, 46, 48] where the interaction energy in the center of the BEC remains large during the expansion and where the reflection coefficient from a single modulation of the disordered potential is of the order of unity. In this case, our numerical results reproduce the strong suppression of the transport of the BEC as observed in the experiments of Refs. [45, 46, 48]. We analyze the scenario of *disorder-induced trapping* proposed in Ref. [45] in which two regions of the BEC are identified. The first region corresponds to the center, where the trapping results from a competition between the interactions and the disorder. The second region corresponds to the tails of the BEC where almost free particles are multiply scattered from the modulations of the disordered potential. There, localization is rather due to the competition between the kinetic energy and the disordered potential but is ultimately due to the almost total classical reflection of the matterwave from a single barrier. These two effects are responsible for blurring Anderson localization effects [45, 46].

Weak disorder corresponds to a situation where the probability of large and wide modulations of the disordered potential is small. In this case, we show that *Anderson localization* does occur as a result of multiple quantum scattering from the modulations of the disordered potential. Let us briefly describe the scenario first proposed in Ref. [25]. Initially, the repulsive interactions are important as compared to the kinetic energy and to the potential energy associated to the disordered potential. Then, the interactions induce the expansion of the BEC and determine the momentum distribution of the BEC. After a time typically equal to the inverse of the initial trapping frequency, the interactions vanish and the momentum distribution reaches a steady state. Then, the BEC is a superposition of non-interacting waves of momentum  $k$ . Each wave localizes with its own localization length  $L_{\text{loc}}(k)$ . By calculating analytically the superposition of the localized waves, we show that the BEC can be exponentially localized or only show an algebraic decay depending on the correlation function of the disordered potential. In particular, due to peculiar long-range correlations, the BEC localizes exponentially in speckle potentials only if  $\xi_{\text{in}} > \sigma_{\text{R}}$ , where  $\xi_{\text{in}}$  is the initial healing length of the BEC and  $\sigma_{\text{R}}$  is the correlation length of the disorder.

### 1.3. Organization of the paper

The paper is organized as follows. In section 2, we review the properties of a BEC at equilibrium in a combined harmonic plus disordered potential, in particular in the non-trivial regime where the healing length of the BEC exceeds the correlation length of the disordered potential. The next two sections deal with the expansion of an interacting

BEC in a disordered potential. Section 3 is devoted to the case of strong disorder. We reproduce and complete our previous results [45] which demonstrate the suppression of the expansion of the BEC in a speckle potential with similar parameters as in the experiments of Refs. [45, 46, 48]. The scenario of disorder-induced trapping is analyzed and characteristic properties of the BEC trapped by the disorder are calculated analytically and compared to numerical results. In particular we derive an analytic expression for the central density of the BEC trapped by disorder which happens to be characteristic of the disorder-induced trapping phenomenon and we show that the ultimate suppression of the expansion of the BEC is due to classical reflections from the large modulations of the disordered potential. We also compare these findings with the case of a BEC expanding in a periodic potential with similar characteristics as the disordered potential. Section 4 is devoted to the case of weak disorder. We show that Anderson localization can show up in an expanding, interacting BEC under appropriate conditions that are clarified. We show that the localization properties of the density profile crucially depend on both the momentum distribution of the expanding BEC and the correlation function of the disordered potential. In particular, in the case of a speckle potential, we find a 1D *effective mobility edge*. We calculate analytically the expected localization lengths and compare our findings to the results of numerical calculations. Finally in section 5, we summarize our findings and discuss expected impacts of our work on experiments on disordered BECs.

## 2. Condensates at equilibrium in a combined harmonic trap plus disordered potential

### 2.1. Interacting Bose-Einstein condensates in a 1D inhomogeneous potential

We consider a low-temperature 1D Bose gas with short-range atom-atom interactions  $g\delta(z)$  where  $g$  is the 1D coupling constant. The Bose gas is assumed to be subjected to (i) a harmonic potential of frequency  $\omega$  and (ii) an additional inhomogeneous potential  $V(z)$ . In a finite system as considered in this work, assuming weak interactions, *i.e.*  $\bar{n} \gg mg/\hbar^2$  where  $\bar{n}$  is the average density and  $m$  the atomic mass [88, 89], the Bose gas will form a Bose-Einstein condensate even in low-dimensional (*e.g.* 1D) geometries [89]. Hence, we can treat the BEC within the mean-field approach [28, 29] using the Gross-Pitaevskii equation (GPE):

$$i\hbar\partial_t\psi(z,t) = \left[ \frac{-\hbar^2\partial_z^2}{2m} + \frac{m\omega^2 z^2}{2} + V(z) + g|\psi(z,t)|^2 - \mu \right] \psi(z,t), \quad (1)$$

where  $\mu$  is the BEC chemical potential.

In the following, we investigate the situations where the additional potential reads  $V(z) = V_R v(z)$  with  $v(z)$  being either a disordered or a periodic function with vanishing average and unity standard deviation. Therefore, we have  $\langle V(z) \rangle = 0$  and  $\sqrt{\langle V(z)^2 \rangle - \langle V(z) \rangle^2} = |V_R|$ . The sign of  $V_R$  depends on the definition of the function  $v(z)$  and on the kind of potential one considers. For instance, in optical speckle potentials, the quantity  $v(z) + 1$  is defined to be positive and  $V_R > 0$  for blue-detuned laser light (case of the experiments of Refs. [45, 48, 79]) while  $V_R < 0$  for red-detuned laser light (case of the experiments of Refs. [44, 46, 80]). For a sine-periodic potential, using  $V_R < 0$  or  $V_R > 0$  does not change the physics. See Appendix A for details.

2.2. The Bose-Einstein condensate wavefunction

Here, we briefly discuss the influence of an inhomogeneous potential on the BEC at equilibrium in the harmonic trap. We assume that the amplitude of the disordered potential is smaller than the chemical potential of the BEC ( $V_R \ll \mu$ ) and that  $\mu \gg \hbar\omega$ . This question has been investigated in details in Ref. [74]. Here, we only outline the results.

At equilibrium, the BEC wavefunction is real (up to an irrelevant uniform phase) and is the solution of Eq. (1) with  $\partial_t \psi = 0$ :

$$\mu\psi(z) = \left[ \frac{-\hbar^2 \partial_z^2}{2m} + \frac{m\omega^2 z^2}{2} + V(z) + g|\psi(z)|^2 \right] \psi(z). \quad (2)$$

For  $V_R = 0$  and  $\mu \gg \hbar\omega$ , the kinetic term can be neglected (Thomas-Fermi regime [29]) and the BEC wavefunction is  $\psi_0(z) = \sqrt{n_0(z)}$  with

$$n_0(z) = \frac{\mu - m\omega^2 z^2/2}{g}. \quad (3)$$

for  $z$  such that  $\mu > m\omega^2 z^2/2$  and  $n_0(z) = 0$  elsewhere. The density profile  $n_0(z)$  is an inverted parabola of length  $L_{\text{TF}} = \sqrt{2\mu/m\omega^2}$  much larger than the healing length  $\xi_{\text{in}} = \hbar/\sqrt{4m\mu}$  [29] (notice that this definition is different from the one of Ref. [74], where we used  $\xi = \sqrt{2}\xi_{\text{in}}$ ).

In the presence of an inhomogeneous potential ( $V_R \neq 0$ ), the parabolic shape of the density profile is perturbed. In general, the kinetic term cannot be neglected any longer. In particular, when  $\xi_{\text{in}} \gtrsim \sigma_R$ , the short-range modulations of the potential  $V(z)$  induce short-range modulations of the BEC wavefunction which contribute significantly in Eq. (2) through the kinetic term. In order to take into account the effect of the inhomogeneous potential, we use a perturbative approach along the lines of Ref. [74]: we write  $\psi(z) = \psi_0(z) + \delta\psi(z)$  with  $\delta\psi \ll \psi_0$ . The first order term of the perturbation series of Eq. (2) is governed by the equation

$$-(\xi_{\text{in}}^0)^2 \partial_z^2 (\delta\psi) + \delta\psi = -\frac{V(z)\psi_0}{2gn_0}, \quad (4)$$

where  $\xi_{\text{in}}^0 = \xi_{\text{in}}/\sqrt{1 - (z/L_{\text{TF}})^2}$  is the local healing length. Since  $L_{\text{TF}} \gg (\xi_{\text{in}}, \sigma_R)$ , it is legitimate to use the local density approximation (LDA) [29], *i.e.* in a region smaller than  $L_{\text{TF}}$ , the quantity  $n_0$  can be considered as uniform. In this approximation, the solution of Eq. (4) is easily found by turning to the Fourier space. We find  $\delta\psi(q) = -\tilde{V}(q)\psi_0/2gn_0$  where

$$\tilde{V}(q) = \frac{V(q)}{1 + (q\xi_{\text{in}}^0)^2} \quad (5)$$

and finally,

$$\psi(z) \simeq \psi_0(z) \left[ 1 - \frac{\tilde{V}(z)}{2gn_0(z)} \right], \quad (6)$$

or equivalently,

$$n(z) \simeq n_0(z) - \tilde{V}(z)/g. \quad (7)$$

This solution justifies *a posteriori* the use of a perturbative approach for  $\tilde{V}_R \ll \mu$ , where  $\tilde{V}_R = \sqrt{\langle \tilde{V}(z)^2 \rangle - \langle \tilde{V}(z) \rangle^2}$  is the standard deviation of the potential  $\tilde{V}(z)$ . Notice that the equality  $\langle \tilde{V}(z) \rangle = 0$  directly follows from Eq. (5).

An important consequence of the solutions (6),(7) is that the BEC wavefunction is only weakly perturbed by the inhomogeneous potential  $V(z)$  if  $\tilde{V}_R \ll \mu$ . It follows from Eq. (5) that for  $\xi_{\text{in}} \ll \sigma_R$ ,  $\tilde{V}(z) \simeq V(z)$  and the relative inhomogeneities of the BEC density are  $\delta n/n \sim V_R/\mu \ll 1$ . For  $\xi_{\text{in}} \gtrsim \sigma_R$ , the relative inhomogeneities are even smaller since all Fourier components of  $\tilde{V}$  are smaller than those of  $V$ . More precisely, the effective potential  $\tilde{V}$  is roughly obtained from  $V$  by suppressing the Fourier components with a wavelength smaller than the healing length. In other words, the BEC density does not follow the modulations of the bare disordered potential  $V(z)$  but actually follows the smoother modulations of the *smoothed disordered potential*  $\tilde{V}(z)$ .

Therefore, an interacting BEC *at equilibrium* in a disordered potential is not localized in the sense of Anderson. One may wonder whether this conclusion still holds for stronger disorder or weaker interactions, where the meanfield approach can break down. This question has been addressed in Ref. [75]. It turns out that for very weak interactions, the Bose gas forms a so-called *Lifshits glass* which corresponds to a Fock state of various localized single-particle states. These states belong to the Lifshits tail of the non-interacting spectrum and are strongly trapped. Therefore, Anderson localization can hardly be observed unambiguously in this case. It seems more favorable to find evidences of Anderson localization in transport experiments of interacting BECs, rather than studying BECs at equilibrium in a disordered trap.

### 3. Strong disorder: Suppression of the expansion of a Bose-Einstein condensate in a speckle potential and disorder-induced trapping scenario

In this section, we investigate the transport properties of a coherent BEC in a disordered potential in the situation of the experiments of Refs. [45, 46, 47, 48]. We thus assume (i) that the chemical potential of the BEC is larger than the depth of the disordered potential ( $\mu > V_R$ ) and (ii) that the correlation length of the disordered potential is much larger than the healing length of the BEC and much smaller than the (initial) size of the BEC,  $\xi_{\text{in}} \ll \sigma_R \ll L_{\text{TF}}$ . We present numerical results which reproduce the suppression of the transport of the BEC in a speckle potential, observed in Refs. [45, 46, 48] and discuss a scenario to explain this phenomenon. In addition, we compare the observed behavior to the case of a periodic potential with similar characteristics.

#### 3.1. Expansion of an interacting BEC in a speckle potential

In order to induce transport, we start from a BEC at equilibrium in the harmonic and disordered potentials (see Sec. 2). At time  $t = 0$ , we suddenly switch off the trapping harmonic potential, keeping the disordered potential. This process is similar to the one used in Refs [45, 46, 48, 85]. The evolution of the BEC is thus governed by the GPE (1) with  $\omega = 0$  and the initial condition corresponds to the TF wavefunction discussed in Sec. 2.2.

The time evolution of the *root mean square* (rms) size of the BEC,  $\Delta z(t) = \sqrt{\langle z^2 \rangle - \langle z \rangle^2}$ , as obtained from the numerical integration of the time-dependent GPE (1), is plotted in Fig. 1 for several amplitudes  $V_R$  of the disordered potential. In the absence of disorder, the interacting BEC expands self-similarly as predicted by

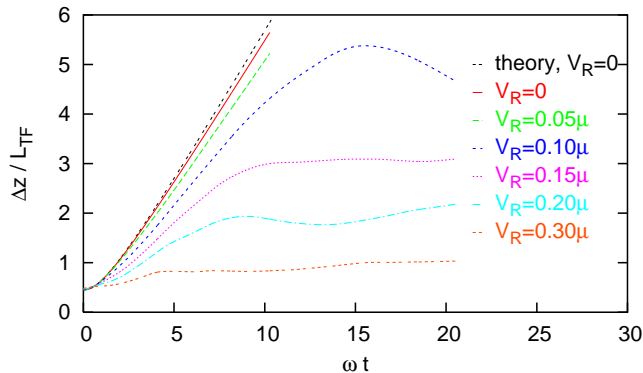


**Figure 1.** (color online) Time-evolution of the rms-size of the BEC wavefunction evolving in the disordered potential  $V$  for several values of the amplitude  $V_R$ . The (black) dashed line is the theoretical prediction of the scaling theory (10) with a vanishing disordered potential. Here, we have used  $\sigma_R = 0.012L_{TF}$  and  $\xi_{in} = 5.7 \times 10^{-4}L_{TF}$ .

the scaling approach [90, 91]:

$$\psi(z, t) \simeq \frac{\psi[z/b(t), 0]}{\sqrt{b(t)}} \exp\left(i \frac{mz^2 \dot{b}(t)}{2\hbar b(t)}\right) \quad (8)$$

where  $b(t)$  is the *scaling parameter* which is governed by the equation

$$\ddot{b}(t) = \omega^2 / b^2(t) \quad (9)$$

with the initial conditions  $b(t=0) = 1$  and  $\dot{b}(t=0) = 0$ . Integrating these equations, we find

$$\sqrt{b(t)(b(t)-1)} + \ln[\sqrt{b(t)} + \sqrt{b(t)-1}] = \sqrt{2}\omega t, \quad (10)$$

which asymptotically reduces to a linear expansion at large time,  $b(t) \sim \sqrt{2}\omega t$ . The numerical calculations agree with this expression as shown in Fig. 1.

The situation is significantly different in the presence of disorder. In this case, the initial BEC wavefunction is the usual Thomas-Fermi inverted parabola perturbed by the disordered potential [74]. For  $t \lesssim 1/\omega$ , the scaling form (8) is still a good solution of the GPE and, according to the scaling theory [90, 91] the BEC wavefunction expands. For larger times and small amplitudes of the disordered potential ( $V_R \lesssim 0.1\mu$ ), the effect of disorder on the expansion observed in the numerical calculations is small and the BEC expands by about one order of magnitude for  $\omega\tau = 10$ . For larger amplitudes of the disorder ( $V_R \gtrsim 0.15\mu$ ), the expansion of the BEC stops after an initial expansion stage described above. This effect signals the localization of the BEC wavefunction due to the presence of disorder.

Important information can be obtained from density profiles of the localized BEC. For instance, density profiles corresponding to a single evolution are plotted at two different times in Fig. 2. From these, it appears that the localized BEC is made of two distinct parts: a static dense core and fluctuating dilute tails (see also Fig.3). In particular, the small fluctuations of  $\Delta z$  observed in Fig. 1 are due to the contribution of the tails of the BEC that still evolve while the core of the wavefunction is localized (see section 3.2).



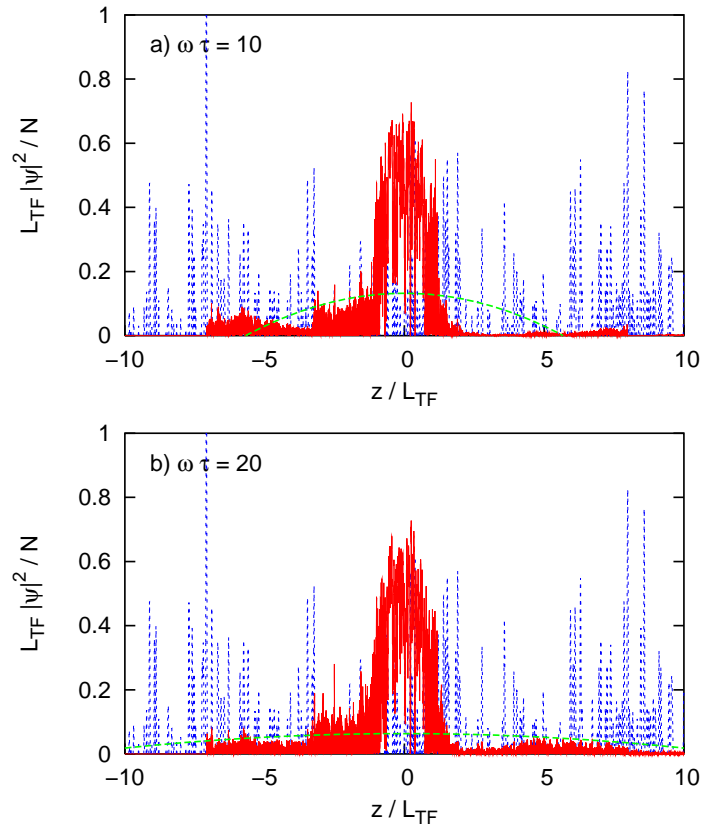


**Figure 2.** (color online) Density profiles of the BEC for  $V_R = 0.2\mu$ ,  $\sigma_R = 0.012L_{TF}$  and  $\xi_{in} = 5.7 \times 10^{-4}L_{TF}$  (solid red lines) for two different values of the expansion time  $\tau$  and expected Thomas-Fermi profiles in the absence of a disordered potential (dashed green lines). We also show the disordered potential normalized so as to be homogeneous to a density ( $V/g$ ; dotted blue line).

It is worth noticing that the BEC expansion stops for amplitudes of disorder significantly smaller than the typical energy per particle in the initial BEC:  $V_R < \mu$ . This *suppression of transport* is phenomenologically similar to what is expected from Anderson localization [8, 9, 10]. Strictly speaking, Anderson localization relies on the existence of localized *single-particle eigenstates* and on the subsequent absence of diffusion [8]. However, we have stressed that the presence of predominant inter-atomic interactions dramatically changes the picture [45]. On one hand, repulsive interactions are expected to reduce the localization effect [74, 92]. During the initial expansion of the BEC, the interaction energy greatly dominates over the kinetic energy in the center of the BEC so that no Anderson-like localization effect is expected in this region. On the other hand, although the particles in the tails are weakly interacting due to the small density, the initial interactions determine their typical energy as the initial expansion stage converts the interaction energy into kinetic energy. We will see that, for strong disorder as considered here, the modulations of the disordered potential will ultimately stop the expansion of the dilute tails, masking any Anderson-like effect (in the case of weak disorder however, Anderson localization can be obtained in this region

as discussed in Sec. 4). In the following, we detail the scenario of *disorder-induced trapping* outlined above and first proposed in Ref. [45].

### 3.2. Scenario of disorder-induced trapping

The dynamics of the BEC in the disordered potential is governed by three different forms of energy: (i) the potential energy associated to the disordered potential, (ii) the interaction energy and (iii) the kinetic energy. It is thus useful to evaluate and compare the kinetic and interaction energies to understand the behavior of the BEC in the disordered potential. To this end, notice first that it follows from the initial expansion of the BEC that the fast atoms populate the tails of the expanding BEC while the slow atoms stay close to the center. In addition, notice that, except for very small amplitudes of the disordered potential and subsequent long expansion times, the density in the core of the BEC remains large whereas it drops to zero in the tails (see Fig. 2). We thus distinguish two different regions of the BEC: (i) the core where the density is large and the interaction energy is dominant and (ii) the tails where the density is small and the kinetic energy dominates. The behavior of the BEC turns out to be completely different in these two regions [45].

*3.2.1. Quasi-static Thomas-Fermi profile in the core of the BEC* - For the sake of clarity, we define the core of the BEC as half the total size of the initial condensate:  $-L_{\text{TF}}/2 < z < L_{\text{TF}}/2$  and call

$$n_c(t) = \frac{1}{L_{\text{TF}}} \int_{-L_{\text{TF}}/2}^{+L_{\text{TF}}/2} dz |\psi(z, t)|^2, \quad (11)$$

the average BEC density in the center. In particular, at time  $t = 0$ , due to the parabolic envelope resulting from the harmonic trap, we find

$$n_c(t = 0) = \frac{11}{12} \frac{\mu}{g} \quad (12)$$

in the absence of disorder but also in the presence of a self-averaging disordered potential $\ddagger$ .

During the initial expansion stage, the average density in the core,  $n_c$ , slowly decreases and the parabolic envelope disappears. Since the interaction energy significantly exceeds the kinetic energy, we expect the local density  $|\psi(z, t)|^2$  to follow almost adiabatically the instantaneous value of  $n_c(t)$  approximately in the Thomas-Fermi regime so that

$$|\psi(z, t)|^2 \simeq n_c(t) - V(z)/g. \quad (13)$$

In order to check this prediction, we plot in Fig. 3a, the result of the numerical integration of the GPE (1) for the density profile in the central region of the BEC during the evolution in the disordered potential at two different times, together with a plot of the analytical expression (13). In particular, two properties are of special interest here. First, we observe that the time-dependent fluctuations of the density profile are significantly smaller than the modulations of the disordered potential  $V(z)/g$ . Second, the density profiles are in good agreement with Eq. (13). This

$\ddagger$  In the context of disordered systems, a quantity is said to be ‘self-averaging’ when it verifies the principle of ‘spatial ergodicity’. In other words, it means that the average over realizations of the disordered potentials of a relevant quantity,  $F$ , equals the corresponding spatial average: *i.e.*  $\langle F \rangle \simeq \frac{1}{L} \int_0^L dz F(z)$ .

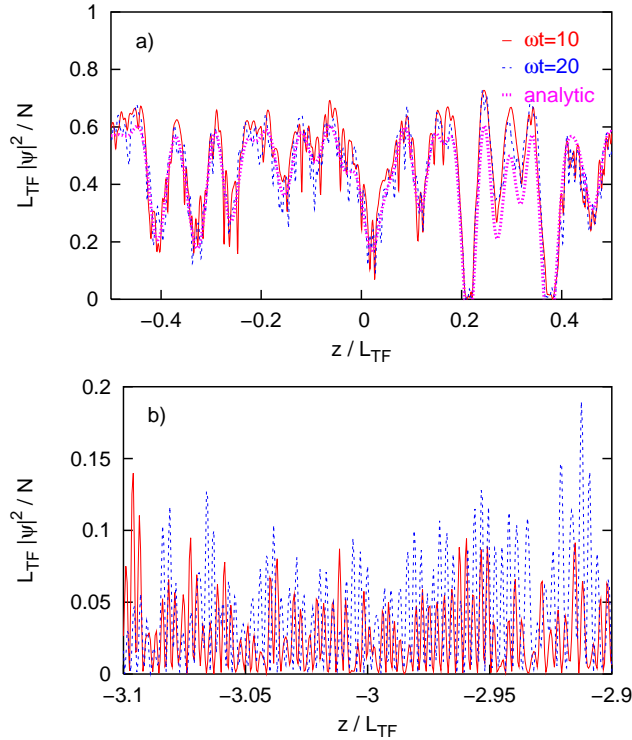


**Figure 3.** (color online) Density profiles of the BEC during the evolution in the disordered potential at different times for  $V_R = 0.2\mu$  in the core (a) and in the tails (b) of the BEC. Both are magnifications of the plots of Fig. 2. The solid (red online) and dashed (blue online) lines correspond respectively to the times  $\omega t = 10$  and  $\omega t = 20$  of the same evolution and the dotted (purple online) line corresponds to Eq. (13) with  $n_c$  as a fitting parameter. Notice the different scales in the two figures.

observation supports the scenario of an adiabatic decrease of the density in the center of the BEC. The value of  $n_c$  at the end of the expansion turns out to be characteristic of this scenario. In the following, we show that  $n_c$  can indeed be computed from the statistical properties of the disordered potential.

The expansion of the core of the BEC in the disordered potential stops when the condensate *fragments*, *i.e.* when the effective chemical potential in the center of the BEC ( $\bar{\mu} = gn_c$ ) decreases down to the value of typically two large modulations of the disordered potential. At this time, the energy per particle in the core of the BEC becomes too small to over-pass the potential barriers and the core of the BEC gets trapped between these large modulations. This scenario allows us to determine the final value of the average density  $n_c$  in the core of the BEC. Let us call  $N_{\text{peaks}}(V)$  the number of maxima of the disordered potential in the central part of the BEC ( $-L_{\text{TF}}/2 < z < L_{\text{TF}}/2$ ) with an amplitude larger than a given value  $V$  and assume that it can be computed from the statistical properties of the disordered potential. The density in the center of the BEC after the trapping has occurred thus corresponds

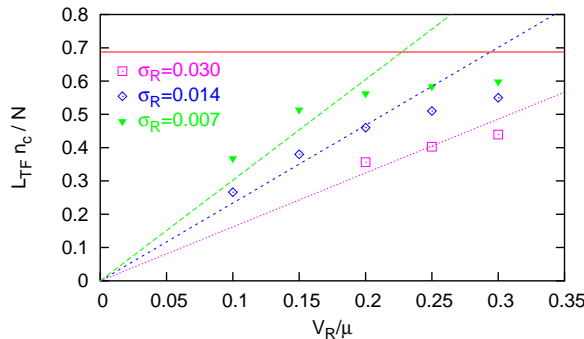


**Figure 4.** (color online) Average density  $n_c$  in the core of the BEC trapped by the disorder versus the amplitude of the disordered potential  $V_R$  for different values of the correlation length  $\sigma_R$  and comparison to Eq. (14). The horizontal (red online) line corresponds to the saturation limit  $n_c = 11\mu/12g$ .

to the maximum value of  $n_c$  below which two modulations of  $V$  in average are present in the center of the BEC. This is simply computed by solving for  $N_{\text{peaks}}(V = n_c g) = 2$ . Although, this scheme is general, it appears clearer when applied to a case where  $N_{\text{peaks}}(V)$  can be explicitly computed. Let us now consider the case of a speckle potential [59, 60] with  $V_R > 0$ . It is shown in Appendix A [see Eq. (A.5)] that in this case  $N_{\text{peaks}}(V) \simeq \alpha \left( \frac{L_{\text{TF}}}{\sigma_R} \right) \exp \left[ -\beta \frac{V}{V_R} \right]$  where  $\alpha \simeq 0.30$  and  $\beta \simeq 0.75$ . From this, we easily find that the final density of the core of the BEC is  $n_c \simeq \frac{1}{\beta} \left( \frac{V_R}{g} \right) \ln \left[ \frac{\alpha L_{\text{TF}}}{2\sigma_R} \right]$ . In addition, we notice that the final density cannot exceed the initial density as resulting from an expansion. Therefore Eq. (14) is valid only for  $\frac{1}{\beta} \left( \frac{V_R}{g} \right) \ln \left[ \frac{\alpha L_{\text{TF}}}{2\sigma_R} \right] \lesssim \mu/g$ . In the opposite situation, the BEC is already multiply fragmented at  $t = 0$  and the final density saturates at  $n_c \simeq \frac{11\mu}{12g}$  [see Eq. (12)]. In summary, we expect that the average density of the BEC trapped by the disorder is

$$n_c \simeq \min \left\{ \frac{1}{\beta} \left( \frac{V_R}{g} \right) \ln \left[ \frac{\alpha L_{\text{TF}}}{2\sigma_R} \right], \frac{11\mu}{12g} \right\}. \quad (14)$$

In order to check Eq. (14), we have extracted the averaged central density [see Eq. (11)] from the wavefunctions  $\psi$  calculated numerically for several amplitudes  $V_R$  and correlation lengths  $\sigma_R$  of the disordered potential. In Fig. 4, we plot  $n_c$  as a function of  $V_R$  for several  $\sigma_R$  together with the prediction (14). The results show that Eq. (14) provides a good estimate of the final density  $n_c$  in the core of the BEC. In particular, for small amplitudes of the disorder,  $n_c$  grows linearly with  $V_R$  with a coefficient in agreement with Eq. (14) up to about 10 %. For larger amplitudes of the disorder,  $n_c$  saturates below  $11\mu/12g$  as expected.

This behavior agrees with experimental results for a blue-detuned speckle potential ( $V_R > 0$ ) [48]. It is worth noticing that our scenario is expected to apply also to the case of a red-detuned speckle potential ( $V_R < 0$ ) as used in Ref. [46]. In this case, the fragmentation occurs when  $\bar{\mu} = |V_R|$  independently of the correlation length of disorder (if  $\xi_{\text{in}} \ll \sigma_R$ ). Then, the fragmented BEC is trapped in the small wells of the disordered potential with a typical size  $\sigma_R$  and with a central density  $n_c \simeq |V_R|/g$

(independent of  $\sigma_R$ ). Instead, for a blue-detuned speckle potential as investigated above, the BEC is trapped between large modulations that may be separated by a distance much larger than  $\sigma_R$ . As a consequence the final density at the center is expected to be significantly larger. This is confirmed by the numerical results of Ref. [93].

*3.2.2. Strong reflections in the tails of the BEC* - The situation is completely different in the tails of the BEC. Due to the small atomic density, the kinetic energy now dominates over the interaction energy. The tails are populated by fast moving, weakly interacting atoms that undergo multiple scattering from the modulations of the disordered potential. Ultimately, the trapping of these atoms results from almost total classical reflection on a single large modulation of the disordered potential with an amplitude exceeding the typical energy of a single particle [45, 46]. This scenario is supported by the density profiles plotted in Fig. 2 where one can observe a sharp drop of the atomic density at the edges of the BEC (*i.e.* at positions  $z_{\min} \simeq -7L_{\text{TF}}$  and  $z_{\max} \simeq 8L_{\text{TF}}$  in Fig. 2). Notice that significant drops correspond either (i) to modulations of the disordered potential larger than the initial chemical potential  $\mu$  (*e.g.* at  $z_{\min} \simeq -7L_{\text{TF}}$ ) or (ii) to a concentration of weaker barriers (*e.g.* at  $z_{\min} \simeq -3.5L_{\text{TF}}$ ).

In contrast with the situation in the core of the BEC, it is expected that (i) the density profile does not show a Thomas-Fermi shape and (ii) the local density is not stationary. Both properties agree with our numerical results as shown in Fig. 3b where we plot a magnification of a small region corresponding to the tails of the BEC of Fig. 2. In particular, the shorter modulations of the wavefunction observed in Fig. 3b are due to the kinetic energy of the particles in the tails. This statement is corroborated by the calculation of the energy per particle,  $\epsilon$ . Due to energy conservation, the energy can be computed at the initial time  $t = 0$  (*i.e.* right after releasing the BEC from the trapping potential),  $\epsilon = \frac{1}{N} \int dz |\psi(z)|^2 [V(z) + g|\psi(z)|^2/2]$ . Using Eq. (7), we easily find that

$$\epsilon = \frac{2\mu}{5} \left[ 1 - \frac{15}{8} \left( \frac{V_R}{\mu} \right)^2 \right]. \quad (15)$$

The disordered potential perturbs the energy per particle only at second order in  $V_R/\mu$ , and, for  $V_R \ll \mu$ , we have  $\epsilon \propto \mu$ . From this, we expect that the typical wavelength  $\Lambda$  of the fluctuations in the tails would be of the order of the healing length in the initial condensate, so that  $\Lambda/2\pi \sim \xi_{\text{in}}$ . This is confirmed by the properties of the momentum distribution of the BEC which show two sharp peaks located around  $p \simeq \pm \hbar/\xi_{\text{in}}$ .

### *3.3. Expansion of a condensate in a periodic potential*

Up to this point, our analysis has shown how the competition between inter-atomic interactions and disorder (in the center of the BEC) or between kinetic energy and disorder (in the tails of the BEC) can strongly suppress the coherent transport of an interacting matterwave in a disordered potential. A natural extension of our analysis is to compare these findings to the situation in a periodic potential with similar characteristics (see Appendix A). In the case of a periodic potential, no suppression of transport is expected as no large peak can provide a sharp stopping of the expansion, and obviously, no ‘à la Anderson’ localization should occur.

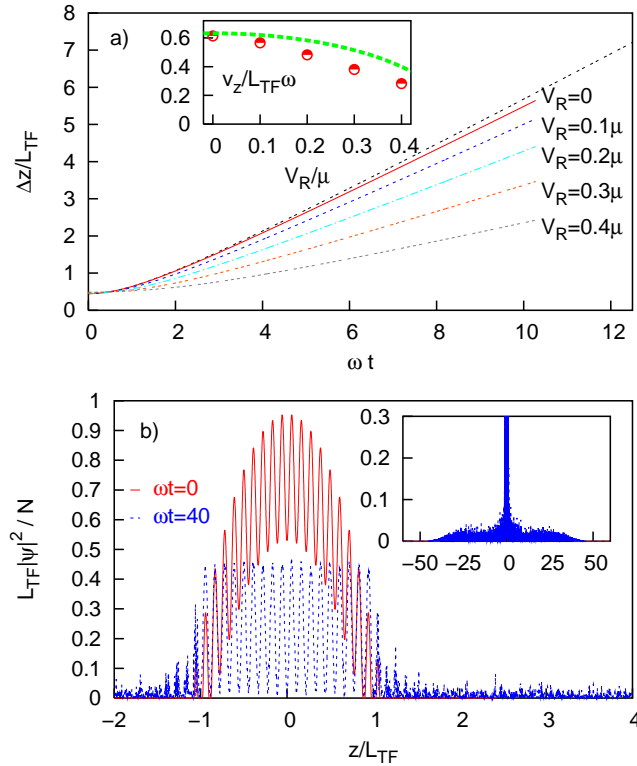


**Figure 5.** (color online) a) Time-evolution of the rms-size of the BEC wavefunction evolving in a periodic potential for several amplitudes  $V_R$  and for  $\lambda = 0.11L_{TF}$ . The theoretical prediction corresponding to Eq. (10) in free space is also shown (black dotted line). The inset shows the velocity of the expansion of the BEC together with the theoretical estimate (17). b) Density profiles of the BEC in the harmonic trap and after an expansion time in the periodic potential of  $t = 40/\omega$  for  $V_R = 0.2\mu$ .

Numerical results for the expansion of the BEC in the periodic potential described in Appendix A.3 are shown in Fig. 5a. The difference with the case of a disordered potential (see Fig. 1) is striking: as expected, the BEC now expands linearly with time with an asymptotic expansion rate that decreases when the amplitude  $V_R$  of the periodic potential increases. A detailed analysis shows however that the transport of the BEC in a periodic potential and in a disordered potential share some properties for the parameters used in this section, as we discuss below.

Again, important information is contained in the density profiles such as the ones plotted in Fig. 5b (to be compared to Fig. 2 which corresponds to the disordered case). Initially ( $\omega t = 0$ ), the density profile follows the modulations of the periodic potential modulated by the parabolic envelope associated to the harmonic trapping [74]. During the initial expansion stage, the density in the center decreases slowly and follows adiabatically a Thomas-Fermi shape with a slowly decreasing instantaneous chemical potential  $\bar{\mu}$ . Then, the evolution of the center stops when the chemical potential  $\bar{\mu}$  exactly matches the potential depth, *i.e.* when the BEC fragments. This

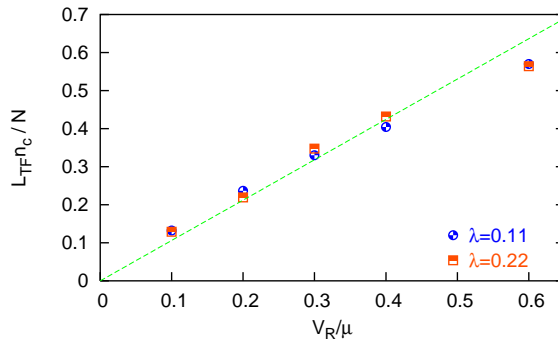


**Figure 6.** (color online) Average density in the center of the BEC trapped in the periodic potential versus the lattice depth  $V_R$  and for two lattice spacings  $\lambda$ . The theoretical prediction (16) is also plotted (green dashed line).

is similar to the disordered case. However, in the case of a periodic potential, it is a deterministic process which appears when

$$n_c \simeq \min \left\{ \sqrt{2} \left( \frac{V_R}{g} \right), \frac{11\mu}{12g} \right\}. \quad (16)$$

As shown in Fig. 6, this formula provides a very good value of the average density in the center of the BEC trapped in the periodic potential. Remarkably, Eq. (16) shows that  $n_c$  does not depend on the lattice spacing  $\lambda$  as confirmed by the numerical results shown in Fig. 6. This is different from the case of a blue-detuned speckle potential ( $V_R > 0$ ) where  $n_c$  has been shown to depend explicitly on the correlation length of the disordered potential [see Eq. (14) and Fig. 4].

During the subsequent evolution, a part of the BEC is thus trapped in the center while the tails still expand as shown in Fig. 5. Let us focus now onto the tails of the BEC. To do so, let us first write the BEC wavefunction  $\psi = \psi_C + \psi_W$  where  $\psi_C$  and  $\psi_W$  account for the center ( $|z| < L_{TF}$ ) and for the tails ( $|z| > L_{TF}$ ) respectively. As the supports of  $\psi_C$  and  $\psi_W$  are spatially separated, we have  $\Delta z^2 = \int dz z^2 |\psi_C|^2 + \int dz z^2 |\psi_W|^2$ . The center gets trapped after a transient time so that  $\int dz z^2 |\psi_C|^2$  tends to a constant,  $\Delta z_0^2$ , at large times. In contrast, the tails expand so that their density decrease. After a typical time  $1/\omega$ , a substantial part of the interaction energy is converted into kinetic energy and the interaction term can be neglected for the subsequent dynamics. We also neglect the periodic potential which has a small amplitude compared to the typical energy per particle in the tails. Now, in free space,  $\Delta z_W^2 = \frac{1}{N} \int dz z^2 |\psi_W|^2 \simeq \frac{2E_W}{Nm} t^2$  at large times where  $E_W$  is the total (kinetic) energy in the tails of the BEC. Due to the conservation of the total energy during the expansion, we have  $N\epsilon = E_C + E_W$  where  $\epsilon$  is the energy per particle given by Eq. (15), and the energy in the center of the BEC,  $E_C = V_R^2 L_{TF}/g$ , is easily computed from the Thomas-Fermi profile in the center of the BEC [see Eq. (13)]. We finally find that  $E_W/N \simeq \frac{2\mu}{5} \left[ 1 - \frac{15}{4} \left( \frac{V_R}{\mu} \right)^2 \right]$  so that  $\Delta z^2 \simeq \Delta z_0^2 + v_z^2 t^2$  at times larger

than  $1/\omega$  with

$$v_z \simeq \sqrt{\frac{2}{5}} \omega L_{\text{TF}} \left[ 1 - \frac{15}{4} \left( \frac{V_{\text{R}}}{\mu} \right)^2 \right]^{1/2}. \quad (17)$$

In the absence of disorder ( $V_{\text{R}} = 0$ ), Eq. (17) is consistent with the scaling theory [Eq. (10)] for which  $\Delta z(t) = b(t)L_{\text{TF}}/\sqrt{5}$ . In the presence of disorder, it provides a reasonable agreement with the numerical findings as shown in the Inset of Fig. 5a. We attribute the discrepancy at the largest values of  $V_{\text{R}}$  to the main two approximations that have been used. First, a strict separation between the tails and the center at  $z = L_{\text{TF}}$  has been used to compute  $E_{\text{W}}$  and we have thus neglected the small intermediate region. Second, the interaction of the atoms with the periodic potential is expected to increase the inertia of the expanding gas and this should contribute to slightly lower the expansion velocity compared to the prediction (17).

#### 4. Weak disorder: Onset of Anderson localization in the expansion of a condensate

In section 3, we have shown that in the experimental conditions of Refs. [45, 46, 48], Anderson localization effects are blurred in an expanding, interacting BEC owing (i) to important repulsive interactions in the center of the BEC, and (ii) to strong reflections from single barriers of the disordered potential in the tails of the BEC. Both effects are related to the presence of large modulations of the disordered potential. It thus appears necessary to work in a parameter range where the probability of single large modulations of the disorder is negligible in order to observe unambiguous Anderson localization of an expanding BEC.

In this section, we work within the regime of weak disorder [a precise definition is given below, see Eq. (21)]. Following the theory of Ref. [25], we show that in this situation, Anderson localization of an interacting BEC can be observed under appropriate conditions that we identify precisely [25]. We consider both cases of an impurity model of disorder and of a speckle potential. In particular, for a speckle potential, we show that the long-range correlations induce a 1D *effective mobility edge*, *i.e.* strong exponential localization is obtained only for  $\xi_{\text{in}} > \sigma_{\text{R}}$ .

##### 4.1. General model of Anderson localization of an expanding Bose-Einstein condensate

*Expansion of a Bose-Einstein condensate* - Let us examine again the expansion of the BEC in the disordered potential (see section 3.1). For weak disorder, the initial interaction energy strongly exceeds the potential energy associated with the disorder so that the first stage of expansion of the BEC is hardly affected by the disorder. For instance, the numerical results of Fig. 1 for  $V_{\text{R}} = 0.5\mu$  and  $V_{\text{R}} = 0.1\mu$  confirm this assertion for durations of expansion up to about  $t \simeq 10/\omega$ . Within this time window, the momentum distribution of the expanding BEC can thus be approximated to that of a BEC expanding in free space [see Eq. (8)]. Calculating the Fourier transform of the scaling solution for interacting BECs expanding in free space,  $\psi(z, t)$ , using the stationary phase approximation (valid for  $t \gg \hbar/\mu$ ), we find the momentum



distribution

$$\mathcal{D}(k, t) \simeq \frac{3N\xi_{\text{in}}/4}{\sqrt{1-1/b(t)}} \times \left[ 1 - \left( \frac{k\xi_{\text{in}}}{\sqrt{1-1/b(t)}} \right)^2 \right] \times \Theta \left[ 1 - \left( \frac{k\xi_{\text{in}}}{\sqrt{1-1/b(t)}} \right)^2 \right] \quad (18)$$

where  $\Theta$  is the Heaviside step function. Since  $b(t) \simeq \sqrt{2}\omega t$ , the momentum distribution reaches a steady-state at times  $t \gg 1/\omega$ :

$$\mathcal{D}(k) \simeq \frac{3N\xi_{\text{in}}}{4} \times [1 - (k\xi_{\text{in}})^2] \times \Theta [1 - (k\xi_{\text{in}})^2]. \quad (19)$$

An important feature of the momentum distribution (19) is that it has a high-momentum cut-off at  $k_c = 1/\xi_{\text{in}}$  (see Fig. 7a).

For  $t \gg 1/\omega$ , almost all the initial interaction energy is converted into kinetic energy. Neglecting the effect of disorder at this stage, this property can be obtained from the scaling solution (8) [90, 91]. We find that the interaction energy is  $E_{\text{int}}(t) \simeq E_{\text{int}}(0)/b(t)$ . Then using the property of conservation of the total energy during the expansion, we find that the ratio of the kinetic energy to the interaction energy is  $E_{\text{kin}}(t)/E_{\text{int}}(t) \simeq b(t) - 1$  which is much larger than unity for  $t \gg 1/\omega$ . It follows from this analysis that for times typically larger than  $1/\omega$ , the expanding BEC is a coherent superposition of almost non-interacting plane waves of momentum  $k$ :

$$\psi(z, t) = \int \frac{dk}{\sqrt{2\pi}} \hat{\psi}(k, t) e^{ikz}, \quad (20)$$

the momentum distribution  $\mathcal{D}(k) = |\hat{\psi}(k, t)|^2$  being stationary and determined by the interaction-driven first expansion stage [25].

*Anderson localization of quantum single particles in a correlated disordered potential -*

Therefore, the interaction of each  $k$ -wave with the disordered potential can be treated independently. According to the Anderson theory [8], the  $k$ -waves will exponentially localize as a result of multiple scattering from the modulations of the disordered potential. In other words, each component  $e^{ikz}$  in Eq. (20) will become a localized function  $\phi_k(z)$ , characterized by an exponential decay at large distances:  $\ln |\phi_k(z)| \simeq -\gamma(k)|z|$ , where  $\gamma(k) = 1/L_{\text{loc}}(k)$  is the so-called Lyapunov exponent, and  $L_{\text{loc}}(k)$  is the localization length. The Lyapunov exponent can be calculated analytically in a correlated disordered potential using the phase formalism approach [94] (see also Appendix B). At the lowest order of the Born expansion which is valid provided that  $\gamma(k) \ll k$ , *i.e.* for

$$V_{\text{R}}\sigma_{\text{R}} \ll \frac{\hbar^2 k}{m} (k\sigma_{\text{R}})^{1/2}, \quad (21)$$

we find the Lyapunov exponent

$$\gamma(k) \simeq \frac{\sqrt{2\pi}}{8\sigma_{\text{R}}} \left( \frac{V_{\text{R}}}{E} \right)^2 (k\sigma_{\text{R}})^2 \hat{c}(2k\sigma_{\text{R}}), \quad (22)$$

where  $E = \hbar^2 k^2 / 2m$ , and  $\hat{c}(\kappa) = \int \frac{du}{\sqrt{2\pi}} c(u) e^{i\kappa u}$  is the Fourier transform of the reduced correlation function  $c(u)$  (see Appendix A). A plot of the Lyapunov exponents versus

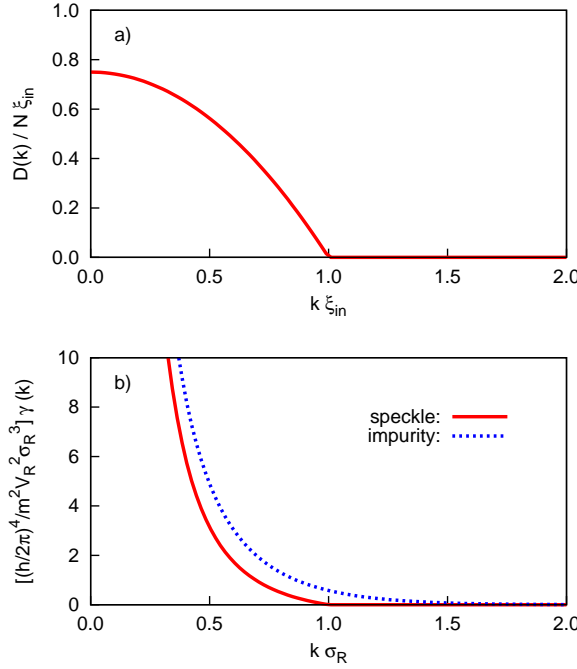


**Figure 7.** (color online) a) Stationary momentum distribution of an expanding, interacting Bose-Einstein condensate at large times ( $t > 1/\omega$ ). b) Lyapunov exponent of single-particles of energy  $E$  as a function of the momentum  $k = \sqrt{2mE}/\hbar$ .

the momentum  $k$  is shown in Fig. 7b for a speckle potential and for a Gaussian impurity model.

Deviations from a pure exponential decay of  $\phi_k$  turn out to be important here. They can be obtained using diagrammatic methods [95, 96], and one finds an integral formula for the average density of each  $k$ -wave:

$$\begin{aligned} \langle |\phi_k(z)|^2 \rangle &= \frac{\pi^2 \gamma(k)}{2} \int_0^\infty du u \sinh(\pi u) \left( \frac{1+u^2}{1+\cosh(\pi u)} \right)^2 \\ &\quad \times \exp\{-2(1+u^2)\gamma(k)|z|\}, \end{aligned} \quad (23)$$

where  $\gamma(k)$  is given by Eq. (22). Notice that at large distances ( $|z| \gg 1/\gamma(k)$ ), Eq. (23) reduces to

$$\langle |\phi_k(z)|^2 \rangle \simeq \left( \frac{\pi^{7/2}}{64\sqrt{2\gamma(k)}} \right) \times \frac{\exp\{-2\gamma(k)|z|\}}{|z|^{3/2}}, \quad (24)$$

so that the exponential decay of the density of the localized single-particle states is corrected by an algebraic decay  $1/|z|^{3/2}$ .

*Anderson localization of the Bose-Einstein condensate* - In the regime of weak disorder defined by condition (21), the Anderson localization transforms each plane

wave  $e^{ikz}$  which appears in the superposition (20) into the localized wave  $\phi_z(z) = r(z) \sin[\theta(z)]$  where  $\theta(z) \simeq kz$  and  $r(z)$  is a slowly decaying envelop (see Appendix B). Therefore, the Fourier transform of  $\phi_k(z)$  is peaked around  $k$ . It follows that the interaction of the  $k$ -wave with the disordered potential only weakly affects the momentum distribution of the BEC. Hence, once each independent  $k$ -wave is localized, the density of the BEC is given by the equation

$$n_0(z) \simeq \left\langle \left| \int \frac{dk}{\sqrt{2\pi}} \hat{\psi}(k, t) \phi_k(z) \right|^2 \right\rangle \quad (25)$$

with  $|\hat{\psi}(k, t)|^2 \simeq \mathcal{D}(k)$ . Assuming that the phases of the functions  $\phi_k(z)$ , which are determined by the local properties of the disordered potential and by the evolution time, are random, uncorrelated functions for different momenta, *i.e.*  $\langle \phi_{k'}^*(z) \phi_k(z) \rangle \simeq 2\pi\delta(k - k')$ , the density of the BEC reduces to

$$n_0(z) \simeq 2 \int_0^\infty dk \mathcal{D}(k) \langle |\phi_k(z)|^2 \rangle \quad (26)$$

where we have used the properties  $\mathcal{D}(k) = \mathcal{D}(-k)$  and  $\langle |\phi_k(z)|^2 \rangle = \langle |\phi_{-k}(z)|^2 \rangle$ . This formula is transparent and contains the main ingredients of the Anderson localization of an interacting BEC in a disordered potential. In a first stage, the interactions drive the expansion of the BEC and determine the momentum distribution  $\mathcal{D}(k)$ . In a second stage, the interactions vanish and the BEC is formed of a superposition of plane waves of energies  $E = \hbar^2 k^2 / 2m$ . Then, each  $k$ -wave localizes with its own localization length  $L_{\text{loc}}(k) = 1/\gamma(k)$ . We will show in the next paragraphs that the precise localization properties of the BEC which are determined by the integral (26), strongly depend on the correlation function of the disordered potential. This is reminiscent of the strong dependence of the single-particle Lyapunov exponent  $\gamma(k)$  on the correlation function.

#### 4.2. Anderson localization of an expanding Bose-Einstein condensate in an impurity model of disorder

Let us consider the case of the impurity model of disorder described in the Appendix A.2. It is made of a series of Gaussian peaks of width  $w$  and amplitude  $V_0$ , all identical and spread randomly along the  $z$  axis. This potential is generic and in the limit  $w \rightarrow 0$  with  $V_0 w$  fixed, we recover the widely used  $\delta$ -correlated (*i.e.* uncorrelated) disorder made of a random series of  $\delta$  peaks used in a number of theoretical investigation of disordered systems [94]. This Gaussian impurity model of disorder can also be implemented using the so-called impurity atom technique with ultracold atomic gases [56, 57]. In this case, the Fourier transform of the reduced correlation function reads

$$\hat{c}(\kappa) = \sqrt{\pi/2} \exp(-\kappa^2/4), \quad (27)$$

and the amplitude and correlation length are  $V_{\text{R}} = \sqrt{\frac{w}{d}} V_0$  and  $\sigma_{\text{R}} = 2w$  respectively (see Appendix A.2). Inserting Eq. (27) into Eq. (22), we find

$$\gamma(k) = \frac{\pi m^2 V_{\text{R}}^2 \sigma_{\text{R}}}{2 \hbar^4 k^2} \exp[-(k \sigma_{\text{R}})^2] \quad (28)$$

which is plotted in Fig. 7b (blue, dotted line).

Using Eqs. (19),(23),(26),(28), we now calculate the density profile of the localized BEC. Since the density profile  $n_0(z)$  is the sum over  $k$  of the functions  $\langle |\phi_k(z)|^2 \rangle$  which decay exponentially with a rate  $2\gamma(k)$ , the long-tail behavior of  $n_0(z)$  is mainly

determined by the  $k$ -components with the smallest  $\gamma(k)$ , *i.e.* those with  $k$  close to the high-momentum cut-off  $k_c = 1/\xi_{\text{in}}$ . Therefore, integrating in Eq. (26) we limit ourselves to the leading order terms in Taylor series for  $\mathcal{D}(k)$  and  $\gamma(k)$  at  $k$  close to  $k_c$ . We find

$$n_0(z) \propto \frac{\exp\{-2\gamma_{\text{eff}}|z|\}}{|z|^{7/2}} \quad (29)$$

$$\text{where } \gamma_{\text{eff}} = \gamma(k = 1/\xi_{\text{in}}). \quad (30)$$

This means that the Anderson localization of an expanding, interacting BEC occurs, provided that the disordered potential is weak enough. In the case of an Gaussian impurity model of disorder, the density profile shows an exponential decay with the effective Lyapunov exponent equal to the one of a single particle of momentum  $k = k_c = 1/\xi_{\text{in}}$  [see Eq. (30)], *i.e.*

$$\gamma_{\text{eff}} = \frac{\pi/32}{\xi_{\text{in}}} \left(\frac{V_{\text{R}}}{\mu}\right)^2 (\sigma_{\text{R}}/\xi_{\text{in}}) \exp[-(\sigma_{\text{R}}/\xi_{\text{in}})^2]. \quad (31)$$

This is a clear characteristics of Anderson localization of the BEC and it can be observed in experiments on ultracold atoms using direct imaging techniques.

#### 4.3. Anderson localization of an expanding Bose-Einstein condensate in a speckle potential

Let us examine now the case of a speckle potential as described in the Appendix A.1 for which, in 1D, the Fourier transform of the reduced correlation (A.4) function reads

$$\hat{c}(\kappa) = \sqrt{\pi/2}(1 - \kappa/2)\Theta(1 - \kappa/2), \quad (32)$$

where  $\Theta$  is the Heaviside step function. The case of a speckle potential is particularly interesting for two reasons. First, it corresponds to the model of disorder used in almost all present experiments with disordered BECs [44, 45, 46, 48, 79, 80]. Second, we will see that speckle potentials offer much richer situations than the impurity model discussed above due to peculiar long-range correlations [25].

One important feature of the speckle potential is the fact that the Fourier transform (32) of the correlation function has a finite support. After Eq. (22), it results that the Lyapunov exponent vanishes for  $k > 1/\sigma_{\text{R}}$ , *i.e.* that strong Anderson localization occurs for non-interacting  $k$ -waves only for  $k < 1/\sigma_{\text{R}}$  [25]. In other words, there is a 1D mobility edge at  $1/\sigma_{\text{R}}$  in the Born approximation. Strictly speaking, higher orders in the Born expansion may provide a non-vanishing Lyapunov exponent for  $k > 1/\sigma_{\text{R}}$ . However, we have shown using direct numerical calculations that the localization length (inverse Lyapunov exponent) for  $k > 1/\sigma_{\text{R}}$  strongly exceeds typical sizes of ultracold atomic samples, so that we can consider  $k = 1/\sigma_{\text{R}}$  as an *effective mobility edge* in our problem [25].

It follows that a part of the expanding BEC (*i.e.* its Fourier components with  $k > 1/\sigma_{\text{R}}$ ) expand to infinity while all the Fourier components with  $k < 1/\sigma_{\text{R}}$  localize exponentially with the  $k$ -dependent Lyapunov exponent

$$\gamma(k) = \frac{\pi m^2 V_{\text{R}}^2 \sigma_{\text{R}}}{2\hbar^4 k^2} (1 - k\sigma_{\text{R}})\Theta(1 - k\sigma_{\text{R}}), \quad (33)$$

found by inserting Eq. (32) into Eq. (22). Equation (33) is plotted in Fig. 7b (solid, red line) and show that for a 1D speckle potential, the high-momentum cut-off  $k_c = \min\{1/\xi_{\text{in}}, 1/\sigma_{\text{R}}\}$  in the integral formula (26) for the BEC density is twofold.

The cut-off  $k = 1/\xi_{\text{in}}$  is related to the momentum distribution of the expanding BEC and is due to the initial atom-atom interactions, while the cut-off  $k = 1/\sigma_{\text{R}}$  is related to the correlation function of the 1D speckle potential and is due to the peculiar finite range correlations of the disordered potential. Now, two very different situations must be distinguished [25].

For  $\xi_{\text{in}} > \sigma_{\text{R}}$ , the high-momentum cut-off  $k_c$  is provided by the momentum distribution. In this case all non-interacting functions  $\langle |\phi_k(z)|^2 \rangle$  are exponentially localized with a finite Lyapunov exponent,  $\gamma(k) \geq \gamma(1/\xi_{\text{in}}) > 0$ . This situation is then similar to the case of the Gaussian impurity model and, integrating Eq. (26), we find

$$n_0(z) \propto \frac{\exp\{-2\gamma_{\text{eff}}|z|\}}{|z|^{7/2}} \quad (34)$$

$$\text{where } \gamma_{\text{eff}} = \gamma(k = 1/\xi_{\text{in}}). \quad (35)$$

Finally, the BEC density profile is exponentially localized with the effective Lyapunov exponent

$$\gamma_{\text{eff}} = \frac{\pi/32}{\xi_{\text{in}}} \left( \frac{V_{\text{R}}}{\mu} \right)^2 (\sigma_{\text{R}}/\xi_{\text{in}})(1 - \sigma_{\text{R}}/\xi_{\text{in}})\Theta(1 - \sigma_{\text{R}}/\xi_{\text{in}}). \quad (36)$$

For  $\xi_{\text{in}} < \sigma_{\text{R}}$ , the situation is completely different. In this case, the cut-off  $k_c$  is provided by the correlation function, and since  $\gamma(k = 1/\sigma_{\text{R}}) = 0$ , the relevant Lyapunov exponents ( $\gamma(k)$  for all  $k < 1/\sigma_{\text{R}}$ ) do not have a finite lower bound. Then, integrating Eq. (26), we find that the BEC density profile is not exponentially localized but rather shows an *algebraic* decay [25]:

$$n_0(z) \propto \frac{1}{|z|^2}. \quad (37)$$

We now present numerical results performed within the Gross-Pitaevskii approximation for the expansion of a BEC in a speckle potential [25]. The inset of Fig. 8 (upper panel) shows that the expansion is strongly suppressed and for long times, the BEC density profile is localized as shown in Fig. 8 (upper panel). Let us discuss now the behavior of the tails.

For  $\xi_{\text{in}} > \sigma_{\text{R}}$ , the density profile obtained numerically is found to be exponentially localized. In addition, fitting the function  $n_0(z) \propto \exp\{-2\gamma_{\text{eff}}|z|\}/|z|^{7/2}$  to the numerical results with the amplitude and  $\gamma_{\text{eff}}$  as fitting parameters, we find that the results for  $\gamma_{\text{eff}}$  are in excellent agreement with the prediction (36) as shown in Fig. 8a (lower panel).

For  $\xi_{\text{in}} < \sigma_{\text{R}}$ , we find that the density profile decays algebraically. We fit the function  $n_0(z) \propto 1/|z|^{\beta_{\text{eff}}}$  with the amplitude and  $\beta_{\text{eff}}$  as fitting parameters, and we find that  $\beta_{\text{eff}} \simeq 2$  in agreement with the prediction (37) as shown in Fig. 8b (lower panel).

## 5. Conclusion and perspectives

In summary, we have theoretically investigated the localization of an expanding 1D BEC with repulsive atom-atom interactions characterized by the initial healing length  $\xi_{\text{in}}$  in a disordered potential of finite correlation length  $\sigma_{\text{R}}$ . We have restricted our study to the regime where the initial interactions of the trapped BEC dominate over the kinetic energy and the disorder, a situation relevant to almost all current experiments with disordered BECs [44, 45, 46, 47, 48, 79, 80]. When the BEC is

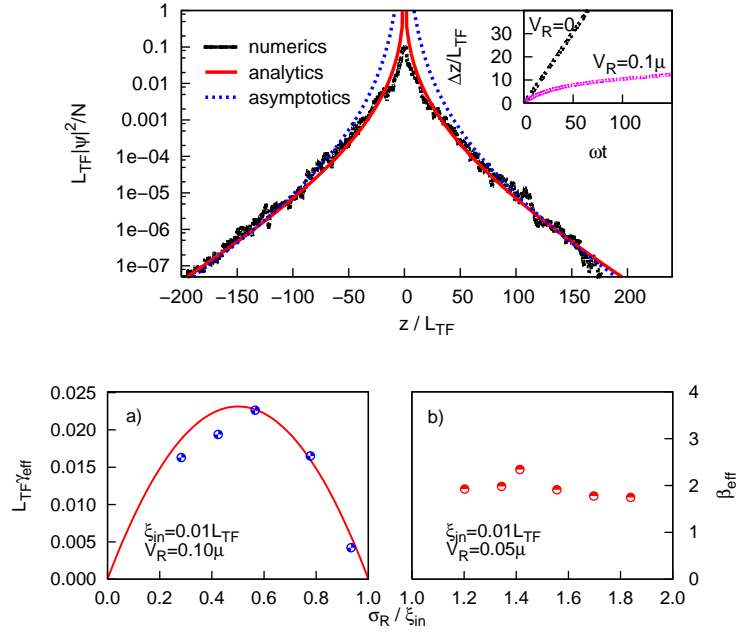


**Figure 8.** (color online) Upper panel: Density profile of the localized BEC in a speckle potential at  $t = 150/\omega$ . Shown are the numerical data (black points), the fit of the result from Eqs. (19), (23) and (26) [red solid line], and the fit of the asymptotic formulas (34),(35) [blue dotted line]. Inset: Time evolution of the rms size of the BEC. The parameters are  $V_R = 0.1\mu$ ,  $\xi_{in} = 0.01L_{TF}$ , and  $\sigma_R = 0.78\xi_{in}$ . Lower panel: a) Lyapunov exponent  $\gamma_{eff}$  in units of  $1/L_{TF}$  for the localized BEC in a speckle potential, in the regime  $\xi_{in} > \sigma_R$ . The solid line is  $\gamma(1/\xi_{in})$  from Eq. (36). b) Exponent of the power-law decay of the localized BEC in the regime  $\xi_{in} < \sigma_R$ . The parameters are indicated in the figure.

released from the trapping potential while keeping the disordered potential on, we find a strong suppression of the expansion, similar to earlier experimental observations [45, 46, 48]. We have shown that this localization effect has completely different causes depending on the strength of the disorder.

*Strong disorder* - The case of strong disorder corresponds to the situation where several modulations of the disordered potential individually are strong-enough to induce an almost total reflection of noninteracting particles of energy equal to the typical expansion energy per particle of the BEC. In particular this case is relevant to the experiments of Refs. [45, 46, 48] and to the numerics of Refs. [45, 93, 97]. In this case, the localization results from a *disorder-induced trapping* [45], whose scenario involves two processes: (i) the fragmentation of the core of the BEC on one hand, and (ii) classical total reflections from single large modulations of the disordered potential on the other hand. In the core of the BEC, the interactions remain important during the initial expansion stage. The BEC is in a quasi-static Thomas-Fermi regime with an effective chemical potential which first slowly decreases during the expansion. When the BEC fragments, the expansion of the core of the BEC stops. In the tails of the BEC, the interactions are negligible and the particles undergo multiple scattering from

the modulations of the disordered potential but the expansion is ultimately stopped by single large modulations. Hence, in the case of strong disorder, the localization is *not* related to Anderson localization.

*Weak disorder* - In the case of weak-enough disorder, the probability of modulations of the disordered potential such that the reflection of a particle of typical energy  $\mu$  approaches unity is negligible, and Anderson localization can show up in an expanding BEC. The scenario is then as follows [25]. In a first stage, the interaction energy dominates over both the kinetic energy and the disorder, and drives the initial expansion of the BEC. After a typical time of  $1/\omega$  where  $\omega$  is the frequency of the initial trapping potential, the interaction energy vanishes and the momentum distribution of the expanding BEC becomes stationary. At this stage, the interactions can be neglected and the BEC wavefunction is a superposition of (almost) non-interacting waves of momentum  $k$ . Each  $k$ -wave Anderson localizes with its own  $k$ -dependent localization length  $L_{\text{loc}}(k)$ . The density profile of the localized BEC is thus the superposition of the localized  $k$ -waves and strongly depends on the correlation function of the disordered potential.

The case of speckle potentials is particularly interesting as the Fourier transform of their correlation function has a finite support. It follows that the localization of the expanding BEC is exponential only for  $\xi_{\text{in}} > \sigma_{\text{R}}$  (in the lowest order of the Born expansion, see Sec. 4). In the opposite situation ( $\xi_{\text{in}} < \sigma_{\text{R}}$ ), the density profile of the BEC decays algebraically as  $1/|z|^2$ . Therefore, for speckle potentials, there is an *effective mobility edge* at  $\xi_{\text{in}} = \sigma_{\text{R}}$  for the Anderson localization of an expanding, interacting BEC [25].

*Perspectives* - Our results suggest that the 1D Anderson localization can be observed in an interacting BEC (initially in the Thomas-Fermi regime) expanding in a disordered potential in experiments similar to those reported in Refs. [45, 46, 48]. We stress that special attention should be paid to using weak-enough disorder to allow the dilution of the BEC during the first expansion stage and to avoid strong reflections from large modulations of the disordered potential. In addition, we have shown that the correlation function of the disordered potential plays a crucial role for the localization properties of the BEC.

However, a couple of challenges have to be taken up to observe Anderson localization in current experiments with expanding BECs. Indeed, in addition to being able to produce long-enough expansions and to measure very small densities, it appears that both disorder and interactions have to be carefully controlled.

In this respect, using disordered potentials created by optical speckle patterns is particularly promising. On one hand, from a practical point of view, the correlation functions of speckle potentials are very well controlled and can be designed almost at will. This allows for a direct comparison between experimental observations and theoretical predictions. On the other hand, for a 1D speckle potential, the Fourier transform of the correlation function has a cut-off at  $k = 1/2\sigma_{\text{R}}$  which induces an *effective mobility edge* at  $k = 1/\sigma_{\text{R}}$  for single-particles and, correspondingly, at  $\xi_{\text{in}} = \sigma_{\text{R}}$  for an expanding, interacting BEC. The presence of this effective mobility edge gives rise to two qualitatively different regimes, which might be observed in experiments, namely *exponential localization* for  $\xi_{\text{in}} > \sigma_{\text{R}}$  and *algebraic decay* of the BEC density profile for  $\xi_{\text{in}} < \sigma_{\text{R}}$ .

Equation (36) shows that for a speckle potential, the stronger localization is obtained for  $\xi_{\text{in}} = 3\sigma_{\text{R}}/2$  and for this value,  $L_{\text{loc}}$  increases with  $\sigma_{\text{R}}$ . It is thus more favourable to work with the shortest correlation length of the disordered potential. To date, correlation lengths about  $\sigma_{\text{R}} \simeq 0.3\mu\text{m}$  have been produced experimentally [48].

The first experiments on the expansion of a BEC in a speckle potential [45, 46, 48] were operated at  $\xi_{\text{in}} \sim \sigma_{\text{R}}/10$ . In order to reach the regime of Anderson localization, it is crucial to lower the interaction energy of the initial condensate in order to increase the healing length  $\xi_{\text{in}}$ . One can either use a Feshbach resonance to directly control the atom-atom interaction strength or lower the density by lowering the number of atoms and/or the radial confinement of the magnetic guide used in Refs. [45, 46, 48]. In the latter case, the dynamics of the expanding BEC in the radial direction can play a role. As the radial confinement is kept during the expansion of the BEC, we expect the radial dynamics be slow compared to the longitudinal expansion. As a result, the radial profile of the BEC would follow adiabatically the local 1D (longitudinal) density, reducing the dynamics to a quasi-1D problem. However, a part of the potential and interaction energies associated to the smooth radial confinement will be converted into longitudinal kinetic energy during the expansion. If the BEC is initially in the 3D Thomas-Fermi regime ( $\mu \gg \hbar\omega_{\perp}$ ), the effective de Broglie wavelength of the 1D expansion can be expected to be  $\lambda_{\text{dB}} \simeq 0.85\xi_{\text{in}}$  to be compared to  $\xi_{\text{in}}$  in the pure 1D case studied here. Hence, for elongated BECs, we do not expect strong differences compared to the 1D situation we have studied in the present work. A more detailed discussion would require further investigation which is beyond the scope of this paper.

We expect that this work will pave the way for the experimental observation of those non-trivial 1D localization properties. This work could also be extended to higher dimensions (namely 2D and 3D geometries) where similar scenarios can be expected but where localization properties would be significantly different.

## Acknowledgments

We are indebted to P. Chavel, D. Gangardt, G.V. Shlyapnikov, M. Lewenstein, J.A. Retter and A. Varon for fruitful discussions. This work was supported by the Centre National de la Recherche Scientifique (CNRS), the Délégation Générale de l'Armement (DGA), the Ministère de l'Enseignement National, de la Recherche et de la Technologie (MENRT), the Agence Nationale de la Recherche (ANR, contract NTOR-4-42586), and the programme QUEDDIS of the European Science Foundation (ESF). The Atom Optics group at LCFIO is a member of the Institut Francilien de Recherche sur les Atomes Froids (IFRAF).

## Appendix A. Random and periodic potentials

In this appendix, we give a couple of details about the inhomogeneous potentials  $V(z)$  to which the atoms are subjected (see section 2.1) *i.e.* a disordered speckle potential, a Gaussian impurity model of disorder and a periodic potential. We plot in Fig. A1 typical realizations of these potentials.

Generally, we write the potential  $V(z)$  as

$$V(z) = V_{\text{R}}v(z/\sigma_{\text{R}}) \quad (\text{A.1})$$

and the spatial auto-correlation function  $C(z) = \langle V(z' + z)V(z') \rangle - \langle V \rangle^2$  as

$$C(z) = V_{\text{R}}^2c(z/\sigma_{\text{R}}) \quad (\text{A.2})$$



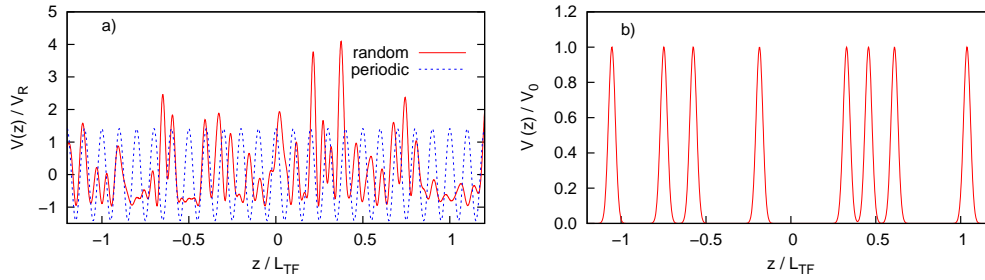


**Figure A1.** (color online) Typical realizations of the potentials  $V(z)$  considered in this work. a) Speckle and periodic potentials: the solid line (red online) shows a typical realization of a disordered speckle potential with  $\sigma_R \simeq 1.39 \times 10^{-2} L_{TF}$  and the dotted line (blue online) shows the periodic potential with  $\lambda = 10^{-1} L_{TF}$ . b) Gaussian impurity model of disorder with  $w = 2 \times 10^{-2} L_{TF}$ .

where  $V_R$  is the typical amplitude of potential,  $\sigma_R$  is the typical space scale (correlation length in the case of disordered potentials) and  $v(u)$  is a given function characteristic of the model of inhomogeneous potential. In this work, we assume that  $\langle v(z) \rangle = 0$  where  $\langle \cdot \rangle$  represents averaging over realizations of disordered potentials or spatial averaging.

#### Appendix A.1. Speckle disordered potential

The main model of disorder we consider is the speckle potential, as it is the one used in many experimental studies of disordered Bose-Einstein condensates [44, 45, 46, 48, 79, 80]. In brief a speckle pattern is formed by diffraction of a laser beam through a rough plate. The intensity of the speckle pattern is proportional to the intensity of the incident laser and the correlation function is determined by the transmission of the diffusive plate [59, 60] (see Ref. [48] for practical realizations in the context of disordered BECs). A disordered potential (*e.g.* a speckle potential) is characterized by its statistical properties, mainly the single-point intensity distribution and the two-point correlation function.

Within the scaling defined above [see Eqs. (A.1),(A.2)], a speckle potential is represented by a random function  $v(u)$  whose single-point statistical distribution is a decaying exponential

$$\mathcal{P}[v(u)] = \exp[-\{v(u) + 1\}] \quad \text{for } v(u) \geq -1 \quad (\text{A.3})$$

and  $\mathcal{P}[v(u)] = 0$  otherwise.

The laser intensity pattern creates an inhomogeneous light shift for the atoms (see Fig. A1a). For a laser which is blue-detuned compared to the atomic resonance line, we have  $V_R > 0$  and for red detuning  $V_R < 0$  [98].

For the numerical calculations presented in the paper, we numerically generate a 1D speckle pattern using a method similar to the one described in Refs. [49, 99] in 1D and corresponding to the following reduced correlation function:

$$c(u) = \text{sinc}(u)^2. \quad (\text{A.4})$$

Another useful characteristics of the speckle potential in the case of blue detuning ( $V_R > 0$ ) is the average number of peaks with an intensity larger than a given value  $V$  within a given region of length  $L_{TF}$  (see section 3.2). Elaborated methods to

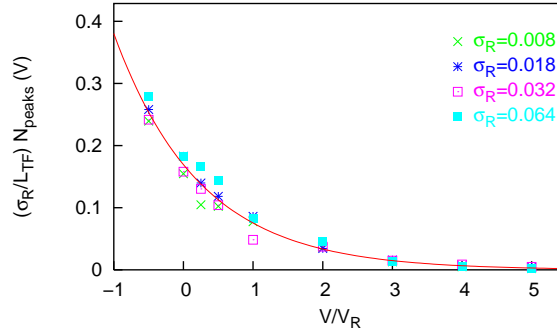


**Figure A2.** (color online) Average number of peaks within a range  $L_{TF}$  with amplitude larger than  $V$  for different values of the correlation length of the disordered potential and comparison to Eq. (A.5).

compute a number of characteristics of speckle potentials can be found in Refs. [59, 60]. Here, we use a simple approximation which suits our purpose. From the probability distribution (A.3), we easily find that the probability density that the local potential is larger than a given value  $V$  is  $P(V) = \exp[-(V+V_R)/V_R]$ . Now, the density of peaks (local maxima of the disordered potential) is  $1/d$  where  $d \propto \sigma_R$  is the typical distance between two peaks. Therefore, typically, the number of peaks  $N_{\text{peaks}}$  within a region of length  $L_{TF}$  with intensity larger than  $V$  scales as  $\frac{L_{TF}}{d} \exp\left(-\frac{V+V_R}{V_R}\right)$ . However, this rough estimate does not take into account the interplay between the local intensity distribution and the finite correlation length of the disordered potential. In the simulated speckle potentials, we find that the typical number of peaks with intensity larger than  $V$  in a  $L_{TF}$ -long region can be approximated by

$$N_{\text{peaks}}(V) \simeq \alpha \left(\frac{L_{TF}}{\sigma_R}\right) \exp\left[-\beta \frac{V+V_R}{V_R}\right] \quad (\text{A.5})$$

with  $\alpha \simeq 0.30$  and  $\beta \simeq 0.75$ , with very good accuracy as shown in Fig. A2.

#### Appendix A.2. Impurity model of disorder

A model of disorder which is very popular in theoretical studies of quantum disordered system is the impurity model [94]:

$$V(z) = V_0 \sum_j g(z - Z_j), \quad (\text{A.6})$$

where  $g$  is a real-valued function peaked at  $z = 0$ , of width  $w$  and such that  $0 \leq g(z) \leq 1$ . The locations of the impurities  $Z_j$  are random and their average distance is denoted  $d$ . The disordered potential is then formed of a series of impurities, all identical but randomly displaced along the  $z$  axis (see Fig. A1b). Here, we consider Gaussian-shaped impurities:

$$g(z) = \exp(-z^2/2w^2). \quad (\text{A.7})$$

This potential can be realized using ultracold atoms (of another species than the BEC) trapped in the Wannier states of the fundamental Bloch band of an optical lattice [56, 57, 100].

From Eq. (A.6), we find that the statistical average of the potential (A.6) is

$$\langle V \rangle = \frac{V_0}{d} \int dx g(x) = \sqrt{2\pi} V_0 \left( \frac{w}{d} \right), \quad (\text{A.8})$$

and the correlation function is

$$C(z) = \frac{V_0^2}{d} \int dx g(x)g(x+z) = V_R^2 c(z/\sigma_R) \quad (\text{A.9})$$

with  $c(u) = \sqrt{\pi} \exp(-x^2)$ ,  $V_R = \sqrt{\frac{w}{d}} V_0$  and  $\sigma_R = 2w$ .

### Appendix A.3. Periodic potential

For periodic potentials (see Fig. A1a), we use

$$V(z) = \sqrt{2} V_R \cos(2\pi z/\lambda) \quad (\text{A.10})$$

corresponding to the mean value  $\langle V \rangle = 0$  and the standard deviation  $\Delta V = |V_R|$ . Such potentials are currently realized using interference patterns of laser beams in geometries with tunable lattice spacings [38, 101].

## Appendix B. Phase formalism for the calculation of Lyapunov exponents in 1D disordered potentials with finite-range correlations

In this section, we outline the phase formalism method used to calculate the Lyapunov exponent (inverse localization length) of a non-interacting particle of energy  $E = \hbar^2 k^2/2m$  in a 1D disordered potential with finite-range correlations [94]. The idea consists in calculating the propagation of the particle using a perturbation on the *phase* of the wavefunction  $\psi(z)$ . Notice that the perturbation is *not* on the wavefunction itself.

The starting point is the Schrödinger equation

$$E\psi(z) = -\frac{\hbar^2}{2m} \frac{d^2}{dz^2} \psi(z) + V(z)\psi(z). \quad (\text{B.1})$$

Without any loss of generality, we can write the wavefunction and its spatial derivative in the form

$$\psi(z) = r(z) \sin[\theta(z)] \quad (\text{B.2})$$

$$\psi'(z) = kr(z) \cos[\theta(z)] \quad (\text{B.3})$$

where  $r(z)$  and  $\theta(z)$  represent the amplitude and the phase of  $\psi(z)$ , respectively. Substituting Eqs. (B.2),(B.3) into Eq. (B.1), we find the coupled equations

$$\theta'(z) = k - \frac{2mV(z)}{\hbar^2 k} \sin^2[\theta(z)] \quad (\text{B.4})$$

$$\ln[r(z)/r(0)] = \int_0^z dz' \frac{mV(z')}{\hbar^2 k} \sin[2\theta(z')] \quad (\text{B.5})$$

Notice that the amplitude  $r(z)$  is not involved in Eq. (B.4). It follows that for weak disorder [see condition (B.9)], it can be solved easily in the lowest order of a perturbation series of the phase  $\theta(z)$ . We write  $\theta(z) = \theta_0 + kz + \delta\theta(z)$  and we find

$$\theta(z) \simeq \theta_0 + kz - \int_0^z dz' \frac{2mV(z')}{\hbar^2 k} \sin^2[\theta_0 + kz'] \quad (\text{B.6})$$

in the Born approximation (lower order). Finally, substituting Eq. (B.6) into Eq. (B.5), we find, in the limit  $|z| \rightarrow \infty$

$$\ln[r(z)/r(0)] = +\gamma(k)|z| \quad (\text{B.7})$$

where  $\gamma(k) = \frac{m}{4\hbar^2 E} \int_{-\infty}^{+\infty} dz C(z) \cos(2kz)$ , where  $C(z)$  is the correlation function of the disordered potential [see Eq. (A.2)] or equivalently

$$\gamma(k) \simeq \frac{\sqrt{2\pi}}{8\sigma_R} \left( \frac{V_R}{E} \right)^2 (k\sigma_R)^2 \hat{c}(2k\sigma_R), \quad (\text{B.8})$$

is the Lyapunov exponent.

Notice that the solution (B.7) corresponds to an exponential *increase* of the envelope of the wavefunction  $\psi(z)$ . In general, the solution of the Schrödinger equation in a disordered potential is the sum of an exponentially increasing function and of an exponentially decaying function. In a finite system, boundary conditions fix the coefficients and one finds true localized states (*i.e.* wavefunctions with an exponentially decaying envelop for both  $z \rightarrow +\infty$  and  $z \rightarrow -\infty$ ). In a time-dependent propagation scheme, the conservation of probability also imposes that the coefficient of the exponentially increasing function vanishes. In the present calculation, since we do not impose boundary conditions, only the exponentially increasing function remains at infinite distance.

In spite of this unimportant limitation, this technique provides a very useful analytic formula for the Lyapunov exponent, valid for any weak 1D disordered potential, possibly with finite-range correlations. An important point is that the phase formalism technique [94] clarifies the Anderson localization effect in 1D disordered potentials. Hence, on small distances (say of the order of  $\sigma_R$ ), the interaction of the wavefunction with the disordered potential induces a small perturbation of the phase  $\theta(z)$  [see Eq. (B.4)], but hardly affect the amplitude  $r(z)$ . Nevertheless, the coupling between the phase and the amplitude [see Eq. (B.5)] is crucial and induces at large distances (say of the order of  $L_{\text{loc}} = 1/\gamma$ ) an exponential envelope, characteristic of Anderson localization. Finally, the non-interacting localized state of energy  $E$  is essentially a plane wave of wavenumber  $k = \sqrt{2mE}/\hbar$  modulated by an exponential envelope. This makes clear the condition of application of the phase formalism approach which requires  $\gamma(k) \ll k$  in order for the phase to be only weakly perturbed. It follows for Eq. (B.8) that this condition reduces to

$$V_R \sigma_R \ll \frac{\hbar^2 k}{m} (k\sigma_R)^{1/2} \quad (\text{B.9})$$

where  $V_R$  is the amplitude and  $\sigma_R$  is the correlation length of the disordered potential.

## References

- [1] H. Risken, *The Fokker-Planck Equation* (Springer, Berlin, 1989).
- [2] A. Aharony and D. Stauffer, *Introduction to Percolation Theory* (Taylor & Francis, London, 1994).
- [3] Y. Imry and S. Ma, Phys. Rev. Lett. **35**, 1399 (1975).
- [4] J.Z. Imbrie, Phys. Rev. Lett. **53**, 1747 (1984).
- [5] J. Bricmont and A. Kupiainen, Phys. Rev. Lett. **59**, 1829 (1987).
- [6] M. Aizenman and J. Wehr, Phys. Rev. Lett. **62**, 2503 (1989).
- [7] M. Aizenman and J. Wehr, Commun. Math. Phys. **130**, 489 (1990).
- [8] P. W. Anderson, Phys. Rev. **109**, 1492 (1958).
- [9] Y. Nagaoka and H. Fukuyama (Eds.), *Anderson Localization*, Springer Series in Solid State Sciences 39 (Springer, Berlin, 1982).

- [10] T. Ando and H. Fukuyama (Eds.), *Anderson Localization*, Springer Proceedings in Physics 28 (Springer, Berlin, 1988).
- [11] B. van Tiggelen, in *Wave Diffusion in Complex Media*, lecture notes at Les Houches 1998, edited by J.P. Fouque, NATO Science (Kluwer, Dordrecht, 1999).
- [12] E. Akkermans and G. Montambaux, *Mesoscopic Physics of Electrons and Photons* (Cambridge University press, 2006).
- [13] T. Giamarchi and H.J. Schulz, Phys. Rev. B **37**, 325 (1988).
- [14] M.P.A. Fisher, P.B. Weichman, G. Grinstein, and D.S. Fisher, Phys. Rev. B **40**, 546 (1989).
- [15] R.T. Scalettar, G.G. Batrouni, and G.T. Zimanyi, Phys. Rev. Lett. **66**, 3144 (1991).
- [16] M. Mézard, G. Parisi, and M.A. Virasoro, *Spin Glass and Beyond* (World Scientific, Singapore, 1987).
- [17] S. Sachdev, *Quantum Phase Transitions* (Cambridge University press, Cambridge, 1999).
- [18] N.W. Ashcroft and N.D. Mermin, *Solid State Physics* (Saunders College Publishing, New York, 1976).
- [19] A.F. Ioffe and A.R. Regel, Prog. Semicond. **4**, 237 (1960).
- [20] N.F. Mott and W.D. Towes, Adv. Phys. **10**, 107 (1961).
- [21] D.J. Thouless, Phys. Rev. Lett. **39**, 1167 (1977).
- [22] E. Abrahams, P.W. Anderson, D.C. Licciardello, and T.V. Ramakrishnan, Phys. Rev. Lett. **42**, 673 (1979).
- [23] F.M. Izrailev and A.A. Krokhin, Phys. Rev. Lett. **82**, 4062 (1999).
- [24] F.M. Izrailev and N.M. Makarov, J. Phys. A: Math. Gen. **38**, 10613 (2005).
- [25] L. Sanchez-Palencia, D. Clément, P. Lugan, P. Bouyer, G.V. Shlyapnikov, and A. Aspect, Phys. Rev. Lett. **98**, 210401 (2007).
- [26] E.A. Cornell and C.E. Wieman, Nobel lectures, Rev. Mod. Phys. **74**, 875 (2002).
- [27] W. Ketterle, Nobel lectures, Rev. Mod. Phys. **74**, 1131 (2002).
- [28] F. Dalfovo, S. Giorgini, L.P. Pitaevskii, and S. Stringari, Rev. Mod. Phys. **71**, 463 (1999).
- [29] L.P. Pitaevskii and S. Stringari, *Bose-Einstein Condensation* (Oxford University press, 2004).
- [30] A.G. Truscott, K.E. Strecker, W.I. McAlexander, G.B. Partridge, and R.G. Hulet, Science **291**, 2570 (2001).
- [31] F. Schreck, L. Khaykovich, K.L. Corwin, G. Ferrari, T. Bourdel, J. Cubizolles, and C. Salomon, Phys. Rev. Lett. **87**, 080403 (2001).
- [32] Z. Hadzibabic, C.A. Stan, K. Dieckmann, S. Gupta, M.W. Zwierlein, A. Görlitz, and W. Ketterle, Phys. Rev. Lett. **88**, 160401 (2002).
- [33] G. Roati, F. Riboli, G. Modugno, and M. Inguscio, Phys. Rev. Lett. **89**, 150403 (2002).
- [34] S. Giorgini, L.P. Pitaevskii, and S. Stringari, arXiv:0706.3360.
- [35] S. Chu, Nobel lectures, Rev. Mod. Phys. **70**, 685 (1998).
- [36] C. Cohen-Tannoudji, Nobel lectures, Rev. Mod. Phys. **70**, 707 (1998).
- [37] W.D. Phillips, Nobel lectures, Rev. Mod. Phys. **70**, 721 (1998).
- [38] G. Grynberg and C. Robilliard, Phys. Rep. **355**, 335 (2000).
- [39] S. Burger, F. S. Cataliotti, C. Fort, F. Minardi, M. Inguscio, M. L. Chiofalo, and M. P. Tosi, Phys. Rev. Lett. **86**, 4447 (2001).
- [40] M. Krämer, L.P. Pitaevskii, and S. Stringari, Phys. Rev. Lett. **88**, 180404 (2002).
- [41] C.D. Fertig, K.M. O'Hara, J.H. Huckans, S.L. Rolston, W.D. Phillips, and J.V. Porto, Phys. Rev. Lett. **94**, 120403 (2005).
- [42] A. Trombettoni and A. Smerzi, Phys. Rev. Lett. **86**, 2353 (2001).
- [43] Th. Anker, M. Albiez, R. Gati, S. Hunsmann, B. Eiermann, A. Trombettoni, and M.K. Oberthaler, Phys. Rev. Lett. **94**, 020403 (2005).
- [44] J.E. Lye, L. Fallani, M. Modugno, D. Wiersma, C. Fort, and M. Inguscio, Phys. Rev. Lett. **95**, 070401 (2005).
- [45] D. Clément, A.F. Varón, M. Hugbart, J.A. Retter, P. Bouyer, L. Sanchez-Palencia, D. Gangardt, G.V. Shlyapnikov, and A. Aspect, Phys. Rev. Lett. **95**, 170409 (2005).
- [46] C. Fort, L. Fallani, V. Guarrera, J. Lye, M. Modugno, D.S. Wiersma, and M. Inguscio, Phys. Rev. Lett. **95**, 170410 (2005).
- [47] T. Schulte, S. Drenkelforth, J. Kruse, W. Ertmer, J. Arlt, K. Sacha, J. Zakrzewski, and M. Lewenstein, Phys. Rev. Lett. **95**, 170411 (2005).
- [48] D. Clément, A.F. Varón, J.A. Retter, L. Sanchez-Palencia, A. Aspect, and P. Bouyer, New J. Phys. **8**, 165 (2006).
- [49] P. Horak, J.-Y. Courtois, and G. Grynberg, Phys. Rev. A **58**, 3953 (1998).
- [50] G. Grynberg, P. Horak, and C. Mennerat-Robilliard, Europhys. Lett. **49**, 424 (2000).
- [51] A.E. Leanhardt, Y. Shin, A.P. Chikkatur, D. Kielpinski, W. Ketterle, and D.E. Pritchard, Phys. Rev. Lett. **90**, 100404 (2003).

- [52] M.P.A. Jones, C.J. Vale, D. Sahagun, B.V. Hall, C.C. Eberlein, B.E. Sauer, K. Furusawa, D. Richardson, and E.A. Hinds, *J. Phys. B* **37**, L15 (2004).
- [53] S. Kraft, A. Günther, H. Ott, D. Wharam, C. Zimmermann, and J. Fortágh, *J. Phys. B* **35**, L469 (2002).
- [54] D. Wang, M. Lukin, and E. Demler, *Phys. Rev. Lett.* **92**, 076802 (2004).
- [55] J. Estève, C. Aussibal, T. Schumm, C. Figl, D. Maily, I. Bouchoule, C.I. Westbrook, and A. Aspect, *Phys. Rev. A* **70**, 043629 (2004).
- [56] U. Gavish and Y. Castin, *Phys. Rev. Lett.* **95**, 020401 (2005).
- [57] B. Paredes, F. Verstraete, and J.I. Cirac, *Phys. Rev. Lett.* **95**, 140501 (2005).
- [58] Ph.W. Courteille, B. Deh, J. Fortágh, A. Günther, S. Kraft, C. Marzok, S. Slama, and C. Zimmermann, *J. Phys. B: At. Mol. Opt. Phys.* **39**, 1055 (2006).
- [59] J.W. Goodman, *Statistical Properties of Laser Speckle Patterns in Laser Speckle and Related Phenomena*, J.-C. Dainty ed. (Springer-Verlag, Berlin, 1975).
- [60] J.W. Goodman, *Speckle Phenomena in Optics: Theory and Applications* (Roberts & Company Publishers, 2007).
- [61] D. Jaksch, C. Bruder, J.I. Cirac, C.W. Gardiner, and P. Zoller, *Phys. Rev. Lett.* **81**, 3108 (1998).
- [62] D. Jaksch and P. Zoller, *Ann. Phys.* **315**, 52 (2005).
- [63] M. Greiner, O. Mandel, T. Esslinger, T.W. Hänsch, and I. Bloch, *Nature (London)* **415**, 39 (2002).
- [64] M. Lewenstein, A. Sanpera, V. Ahufinger, B. Damski, A. Sen(de), and U. Sen, *Avd. Phys.* **56**, 243 (2007).
- [65] R. Roth and K. Burnett, *Phys. Rev. A* **68**, 023604 (2003).
- [66] B. Damski, J. Zakrzewski, L. Santos, P. Zoller, and M. Lewenstein, *Phys. Rev. Lett.* **91**, 080403 (2003).
- [67] L. Fallani, J.E. Lye, V. Guarrera, C. Fort, and M. Inguscio, *Phys. Rev. Lett.* **98**, 130404 (2007).
- [68] A. Sanpera, A. Kantian, L. Sanchez-Palencia, J. Zakrzewski, and M. Lewenstein, *Phys. Rev. Lett.* **93**, 040401 (2004).
- [69] V. Ahufinger, L. Sanchez-Palencia, A. Kantian, A. Sanpera, and M. Lewenstein, *Phys. Rev. A* **72**, 063616 (2005).
- [70] L. Sanchez-Palencia, V. Ahufinger, A. Kantian, J. Zakrzewski, A. Sanpera, and M. Lewenstein, *J. Phys. B: At. Mol. Opt. Phys.* **39**, S121 (2006).
- [71] O. Lenoble, L.A. Pastur, and V.A. Zagrebnov, *C. R. Physique* **5**, 129 (2004).
- [72] G.M. Falco, A. Pelster, and R. Graham, *Phys. Rev. A* **75**, 063619 (2007).
- [73] A. De Martino, M. Thorwart, R. Egger, and R. Graham, *Phys. Rev. Lett.* **94**, 060402 (2005).
- [74] L. Sanchez-Palencia, *Phys. Rev. A* **74**, 053625 (2006).
- [75] P. Lugan, D. Clément, P. Bouyer, A. Aspect, M. Lewenstein, and L. Sanchez-Palencia, *Phys. Rev. Lett.* **98**, 170403 (2007).
- [76] V.I. Yukalov, E.P. Yukalova, K.V. Krutitsky, and R. Graham, *Phys. Rev. A* **76**, 053623 (2007).
- [77] N. Bilas and N. Pavloff, *Eur. Phys. J. D* **40**, 387 (2006).
- [78] P. Lugan, D. Clément, P. Bouyer, A. Aspect, and L. Sanchez-Palencia, *Phys. Rev. Lett.* **99**, 180402 (2007).
- [79] D. Clément, P. Bouyer, A. Aspect, and L. Sanchez-Palencia, arXiv:0710.1984 (2007).
- [80] Y.P. Chen, J. Hitchcock, D. Dries, M. Junker, C. Welford, R.G. Hulet, arXiv:0710.5187 (2007).
- [81] J. Wehr, A. Niederberger, L. Sanchez-Palencia, and M. Lewenstein, *Phys. Rev. B* **74**, 224448 (2006).
- [82] A. Niederberger, T. Schulte, J. Wehr, M. Lewenstein, L. Sanchez-Palencia, and K. Sacha, *Phys. Rev. Lett.* **100**, 030403 (2008).
- [83] R. C. Kuhn, C. Miniatura, D. Delande, O. Sigwarth, and C. A. Müller, *Phys. Rev. Lett.* **95**, 250403 (2005).
- [84] R. C. Kuhn, C. Miniatura, D. Delande, O. Sigwarth, and C. A. Müller, *New J. Phys.* **9**, 161 (2007).
- [85] L. Sanchez-Palencia and L. Santos, *Phys. Rev. A* **72**, 053607 (2005).
- [86] T. Paul, P. Leboeuf, N. Pavloff, K. Richter, and P. Schlagheck, *Phys. Rev. A* **72**, 063621 (2005).
- [87] T. Paul, P. Schlagheck, P. Leboeuf, and N. Pavloff, *Phys. Rev. Lett.* **98**, 210602 (2007).
- [88] M. Olshanii, *Phys. Rev. Lett.* **81**, 938 (1998).
- [89] D.S. Petrov, G.V. Shlyapnikov, and J.T.M. Walraven, *Phys. Rev. Lett.* **85**, 3745 (2000).
- [90] Yu. Kagan, E.L. Surkov, and G.V. Shlyapnikov, *Phys. Rev. A* **54**, R1753 (1996).
- [91] Y. Castin and R. Dum, *Phys. Rev. Lett.* **77**, 5315 (1996).
- [92] D.L. Shepelyansky, *Phys. Rev. Lett.* **73**, 2607 (1994).
- [93] M. Modugno, *Phys. Rev. A* **73**, 013606 (2006).
- [94] I.M. Lifshits, S.A. Gredeskul, and L.A. Pastur, *Introduction to the Theory of Disordered*

- Systems*, (Wiley and sons, New York, 1988).
- [95] A.A. Gogolin, V.I. Mel'nikov, and E.I. Rahba, Sov. Phys. JETP **42**, 168 (1976).
  - [96] A.A. Gogolin, Sov. Phys. JETP **44**, 1003 (1976).
  - [97] E. Akkermans, S. Ghosh, and Z. Musslimani, cond-mat/0610579.
  - [98] R. Grimm, M. Weidemüller, and Yu. B. Ovchinnikov, Adv. At. Mol. Opt. Phys. **42**, 95 (2000); physics/9902072.
  - [99] J.M. Huntley, Appl. Opt. **28**, 4316 (1989).
  - [100] P. Massignan and Y. Castin, Phys. Rev. A **74**, 013616 (2006).
  - [101] L. Fallani, C. Fort, J. Lye, M. Inguscio, Opt. Express **13**, 4303 (2005).